Surface/Interface Scattering

Paul Zschack, NSLS-II/Brookhaven National Lab

X-ray & Neutron School, 23 July 2018

Thoughts before we start…

- A ‘surface’ is actually an interface
- All materials interact with their environment at their surface or interface
- Don’t wish to provide depth, nuance, or detailed derivations, but rather a broad tour of applications that provide a view of what’s possible today.

Interfacial Science

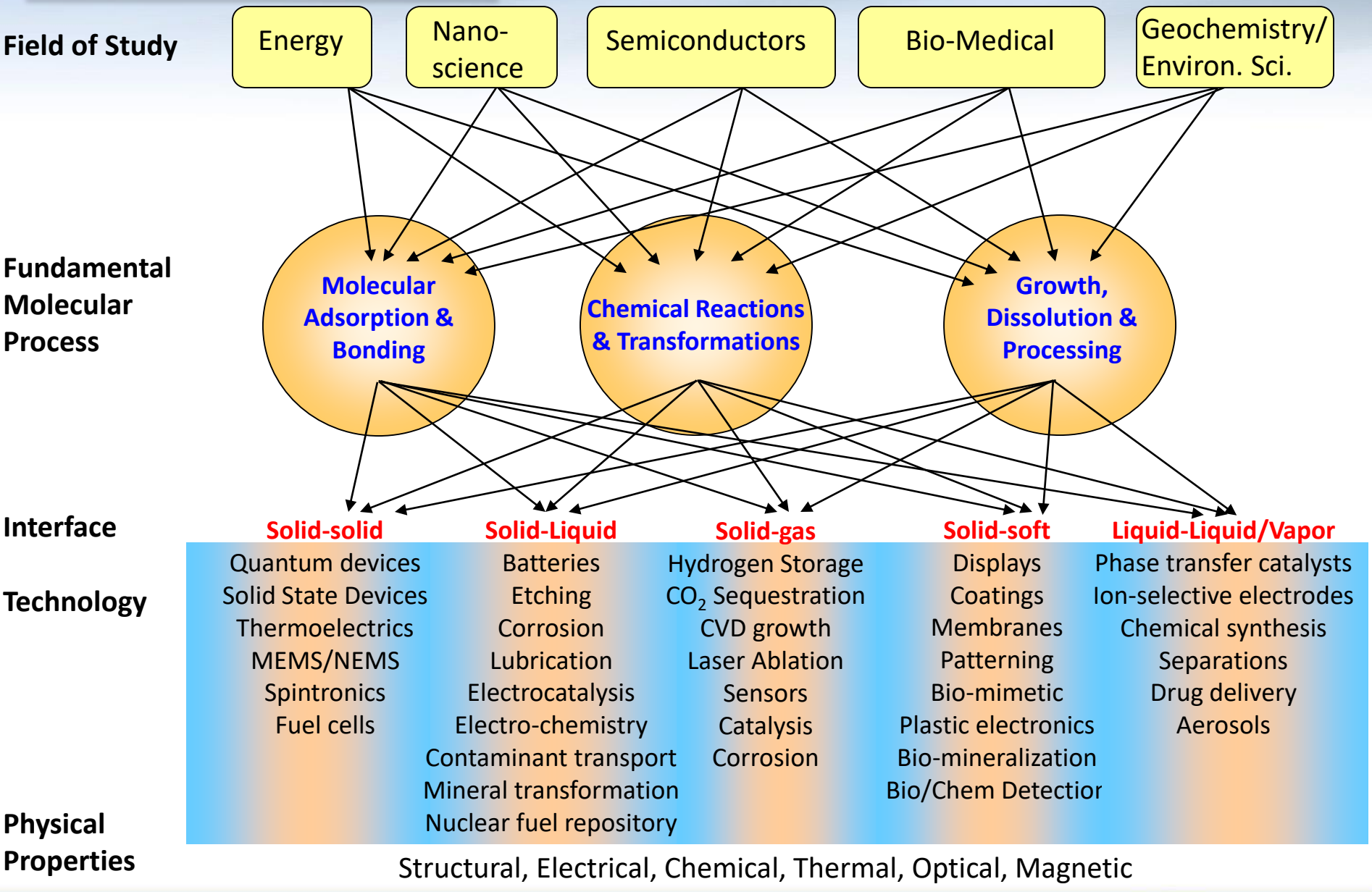

Motivations

- Fundamental understanding
- Technology development
  - Electronics
  - Catalysis
  - Separations
- Materials growth & dissolution principles
- New, novel interface properties
- Environmental remediation
- Nano-science

- Why x-rays?

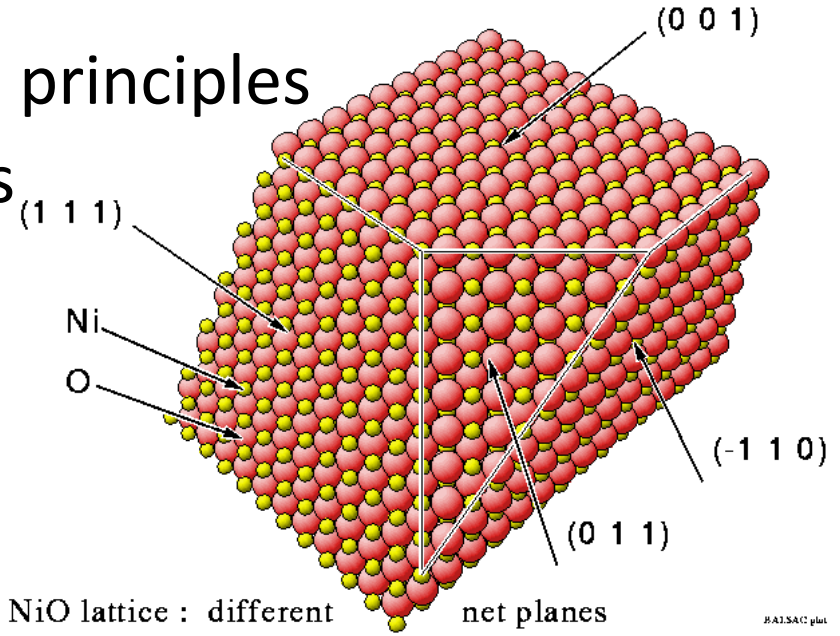

Advantages of using X-Rays

Why x-rays?

- Penetration – In-situ studies possible
- Contrast – elemental sensitivity
- Kinematic – straightforward interpretation

Synchrotrons provide:

- Flux (and brightness)
- Time-resolution
- Tunability

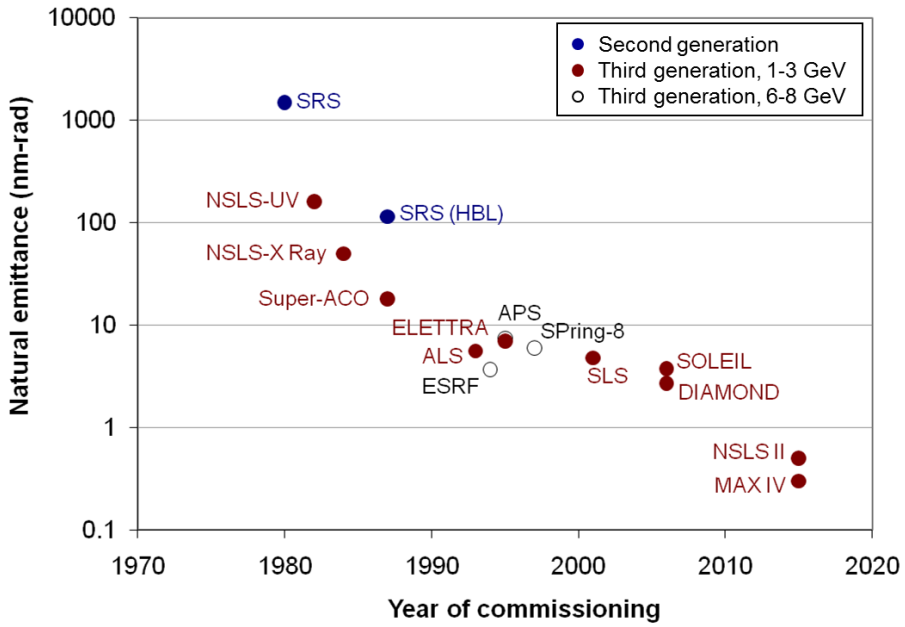

Outline

- Reflectivity
- Diffraction & in-plane structure
- The crystal truncation rod (CTR)
- Interfacial chemistry
- Materials Synthesis using Pulsed Laser Deposition
- Interface Visualization with X-Ray Reflection Interface Microscopy
  - Application to thin-films
- Surface sensitive coherent x-ray scattering (XPCS, CDI)
- Instruments at light sources for interface science

X-ray reflection and refraction

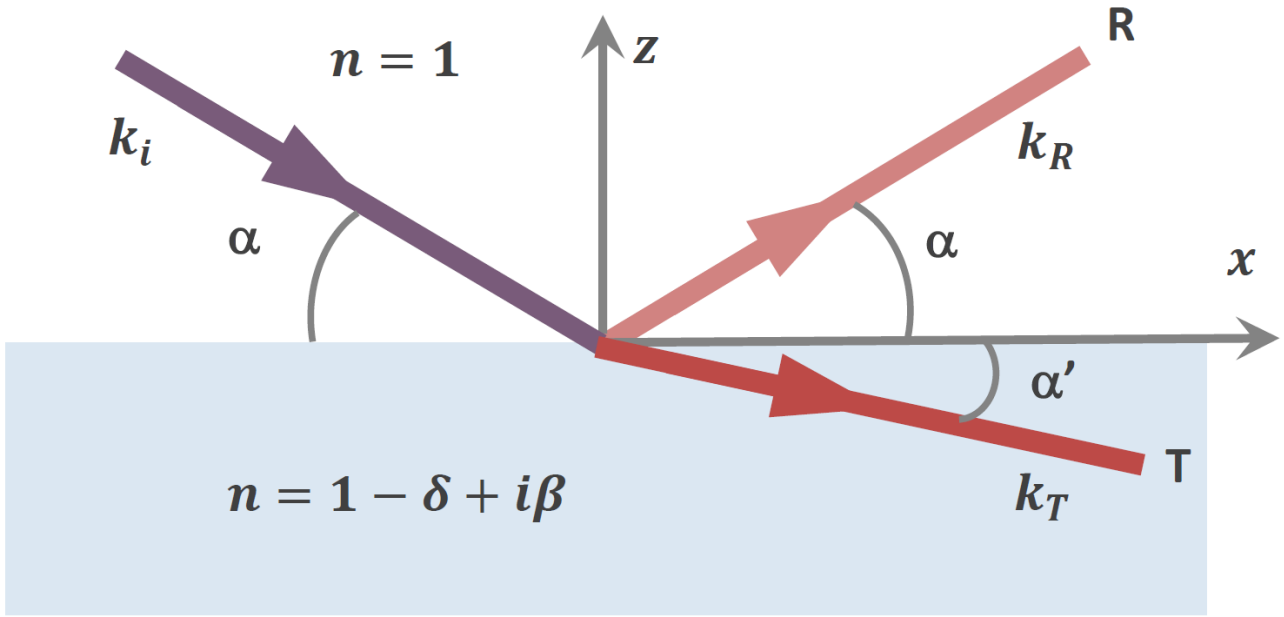

$$n = 1 - \delta + i\beta$$

$$\delta = \frac{\lambda^2}{2\pi} r_e \rho_e$$

$$\beta = \frac{\lambda}{4\pi} \mu_x.$$

Snell's law: $\cos\alpha = n\cos\alpha'$

Critical angle for total external reflection (α'=0): $\alpha_c = \cos^{-1} n \approx \sqrt{2\delta}$

Typical $\delta \sim 10^{-5}$, so $\alpha_c \sim 0.1° - 0.5°$

Wave vector transfer for reflected beam $q_z = 2k\sin(\alpha)$

Reflectivity and transmission

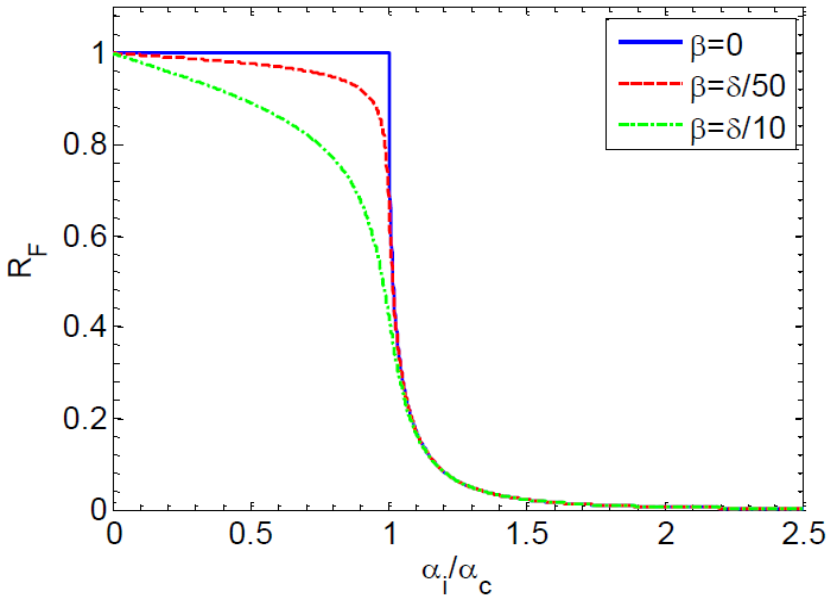

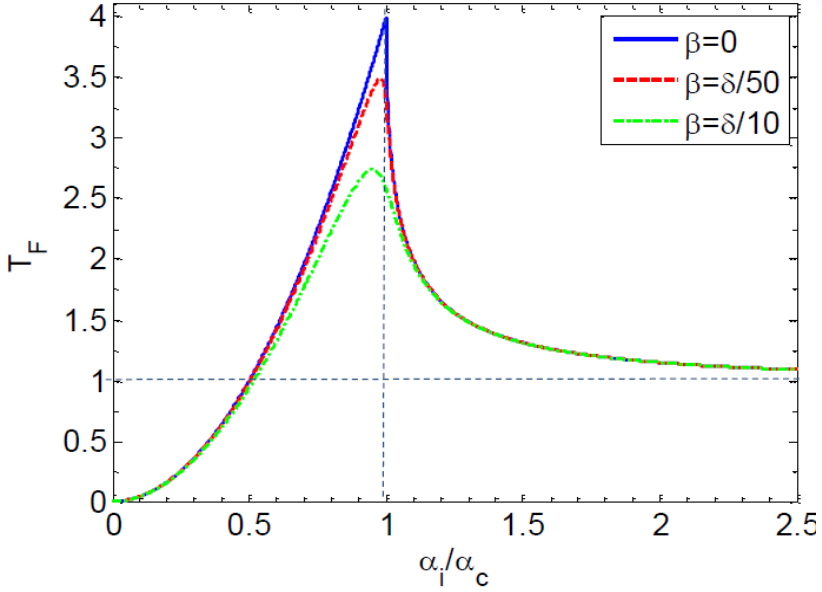

$$T_F = \left| \frac{2\alpha_i}{\alpha_i + \alpha_t} \right|^2 \qquad R_F = \left| \frac{\alpha_i - \alpha_t}{\alpha_i + \alpha_t} \right|^2$$

$$n = 1 - \delta + i\beta$$

$$\delta = \frac{\lambda^2}{2\pi} r_e \rho_e$$

$$\beta = \frac{\lambda}{4\pi} \mu_x.$$

$\cos \alpha_i = \eta \cos \alpha_t$

X-ray reflectivity and penetration depth

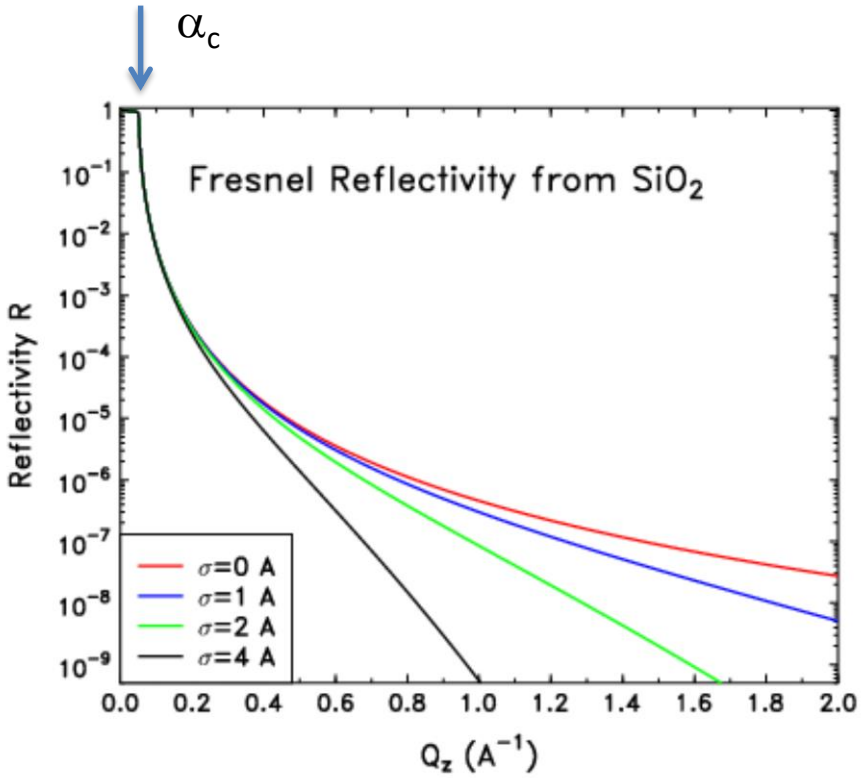

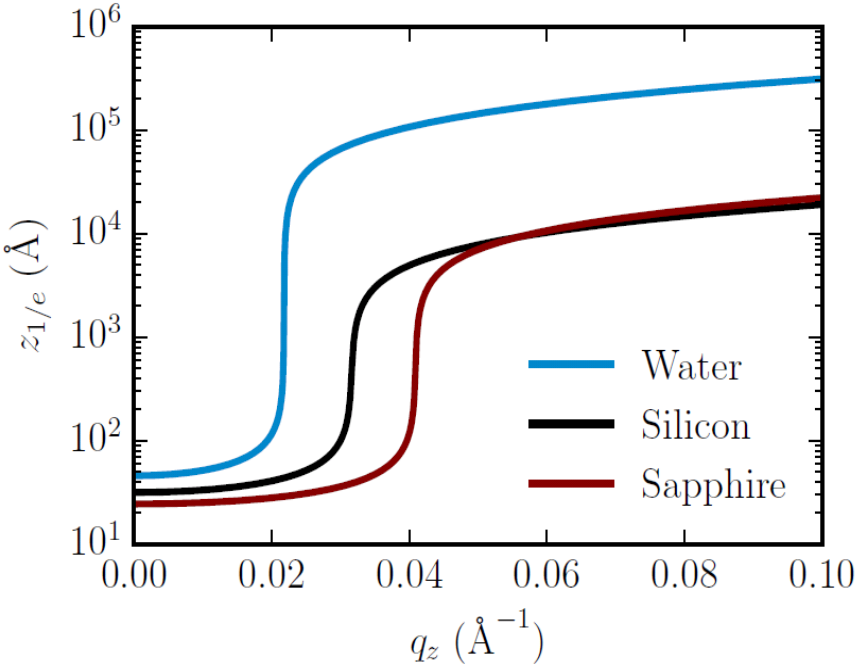

$$r_{rough} = r_{ideal}\, e^{-2k_z k_z' \sigma^2}$$

Surface reconstruction – Si (100) 2x1

- Ideally terminated surface may not be lowest energy state – broken symmetry
- Surface reconstructions are widely observed

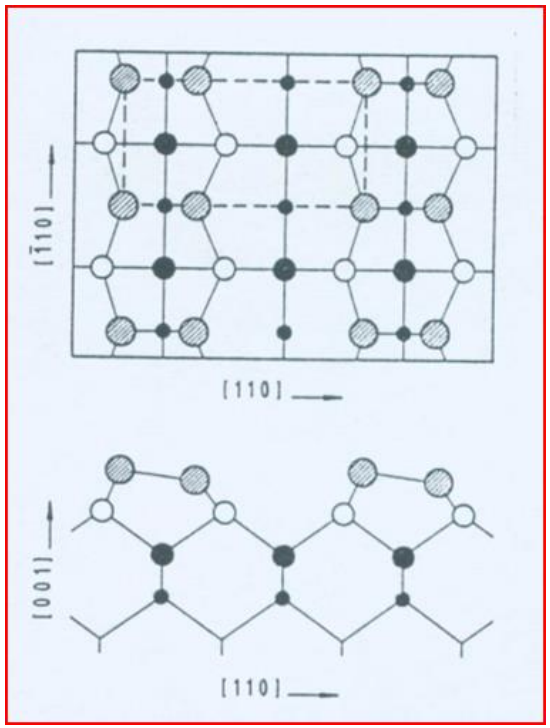

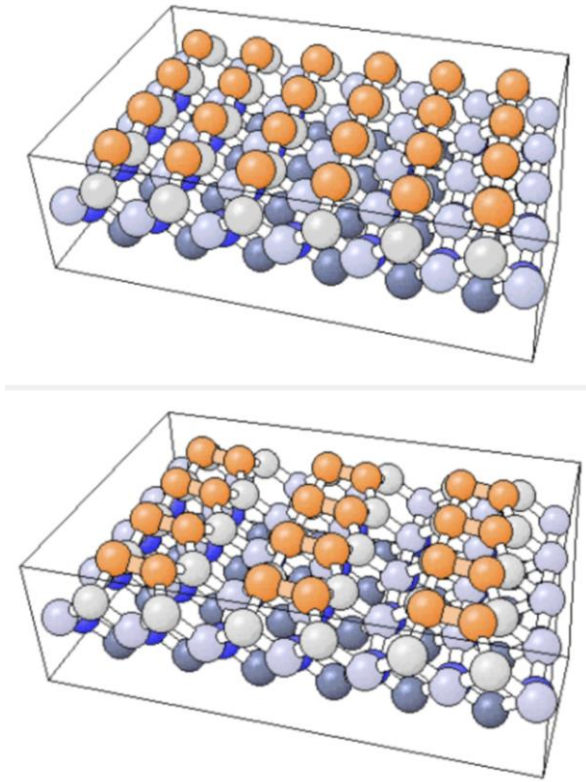

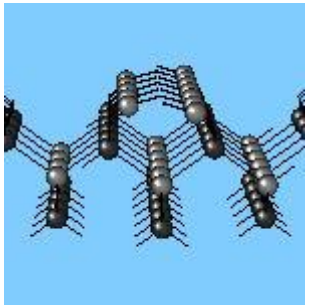

Grazing incidence surface diffraction

- Grazing incidence provides for reduced bulk scattering and high S/N ratio
- In-plane diffraction can be used to measure surface structure factors and solve the surface structure

H. Dosch, Springer Tracts in Mod. Phys. (Springer), Berlin, 1992, p. 126.

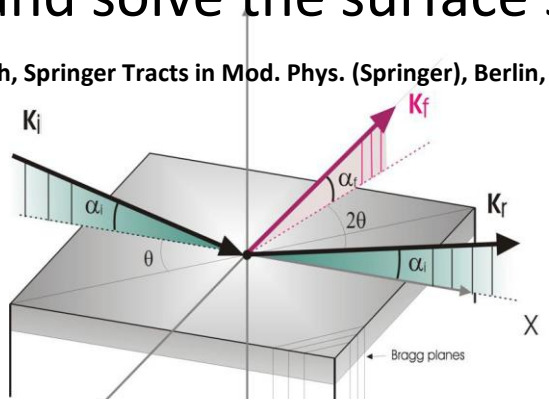

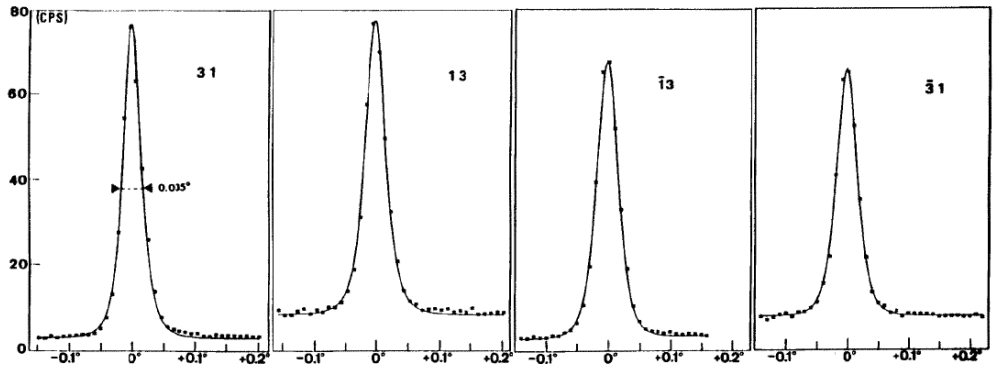

Fig. 3. As/Si(001)2×1 reconstructed surface. Transverse scans of four 31 integer orders with narrow FWHM insensitive to the azimuthal angle. Angular steps: 0.01°

h k	Si(001)2 × 1, 1 × 2		
	F^{obs}	σ	F^{calc}
0 3/2	1.56	0.10	1.55
0 5/2	0.53	0.06	0.50
0 3			
1 1/2	0.82	0.08	0.71
1 1			
1 3/2	0.85	0.05	0.87
1 2	1.72	0.06	1.74
1 5/2			
1 3	0.96	0.07	0.96
1 7/2	0.88	0.04	0.88
1 4			
2 1/2	0.65	0.07	0.76
2 3/2	1.24	0.04	1.20
2 5/2	0.40	0.04	0.43
2 3	1.22	0.11	1.28
3 1/2			
3 3/2			

$\chi^2 = 1.30$

$B_{Si} = 1.0\ (\pm 0.1)$

Patterson synthesis

- Patterson Function corresponds to a map of position vectors (relative positions) between each pair of atoms in the structure.
- The Patterson function is equivalent to the electron density convoluted with its inverse.

$$P(\vec{u}) = \rho(\vec{r}) * \rho(-\vec{r}).$$

$$P(xy) = \frac{1}{a}\sum_{hk} |F_{hk}|^2 \cos[2\pi(hx + ky)]$$

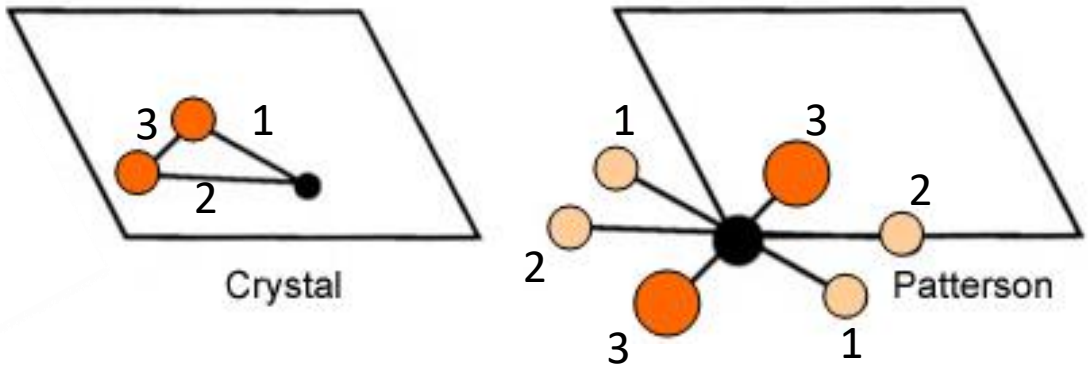

Patterson synthesis (2)

- Large π-conjugated organic molecule adsorbed on a metallic surface (end-capped quaterthiophene on Ag(111))
- Previous belief was that organic molecules absorbed on weakly interacting surfaces remain essentially undistorted
- Result of this study showed significant distortion of the thiophene rings and elongation of the bond distances.

H. L. Meyerheim *et al* 2000 *Europhys. Lett.* **52** 144

Patterson-function $P(u,v)$ for EC4T/Ag(111).

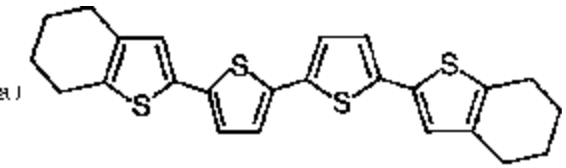

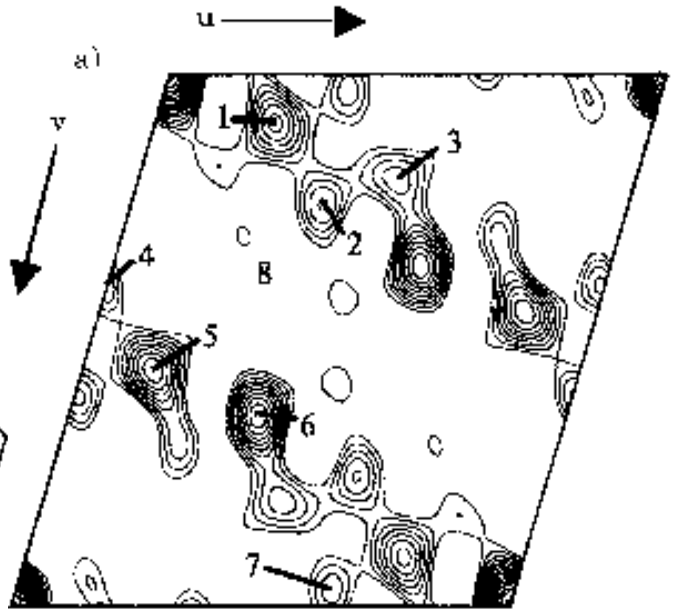

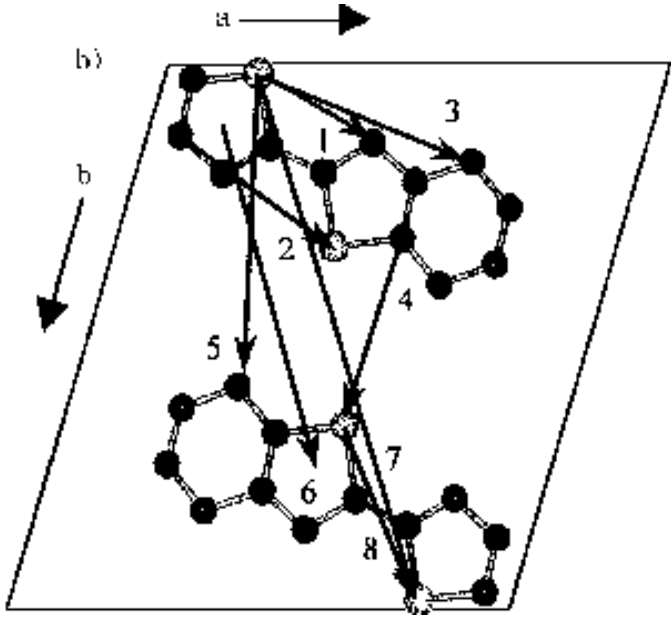

Reciprocal space (Fourier transform)

- Large things in real space are sharp (small) in reciprocal space. So, a large single crystal gives rise to very sharp Bragg peaks.
- Small things in real space are broad in reciprocal space. Very small crystals have broad diffraction peaks.
- A plane in real space is a line in reciprocal space. So the scattering from a 2D plane in real space is a 1-dimensional line in reciprocal space.

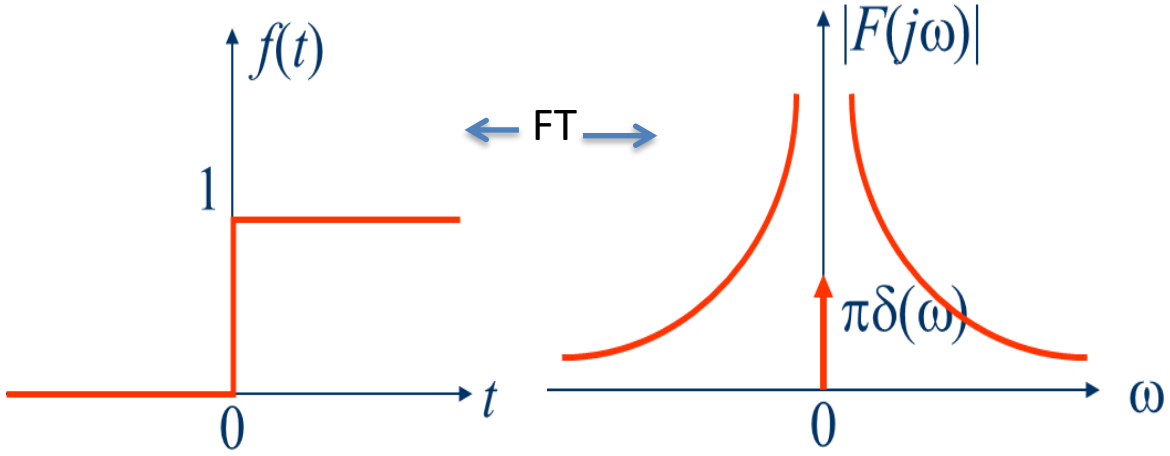

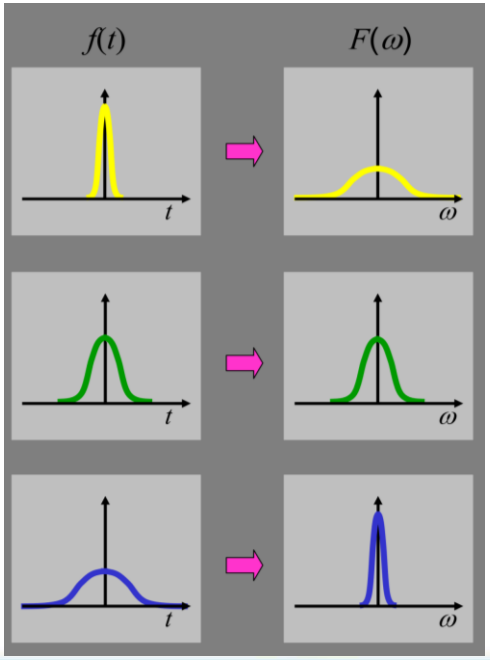

Review of scattering equations

$$E(\mathbf{R}) \propto FT[\rho(\mathbf{r})] = \sum_n f_{a,n} e^{i\,\mathbf{Q}\bullet\mathbf{r}_n}$$

$$I \propto |E|^2$$

$$E \propto \sum_{-(N_1-1)/2}^{(N_1-1)/2} e^{i\,2\pi\, n_1 H} \sum_{-(N_2-1)/2}^{(N_2-1)/2} e^{i\,2\pi\, n_2 K} \sum_{-(N_3-1)/2}^{(N_3-1)/2} e^{i\,2\pi\, n_3 L} \sum_{j=1}^{m} f_{a,j} e^{i\,\mathbf{Q}\bullet\mathbf{r}_j} e^{-M_j}$$

Sum over n_1, N_1 total cells

Sum over n_2, N_2 total cells

Sum over n_3, N_3 total cells

Thermal disorder parameter

Sum over the m atoms in the unit cell

Structure factor of the unit cell

$$F_c = \sum_{j=1}^{m} f_{a,j} e^{i\,\mathbf{Q}\bullet\mathbf{r}_j} e^{-M_j}$$

Slit Function

$$S_1 = \sum_{-(N_1-1)/2}^{(N_1-1)/2} e^{i\,2\pi\, n_1 H} = \frac{\sin(N_1 \pi H)}{\sin(\pi H)}$$

$$\rightarrow N_1 \text{ as } H \rightarrow \text{integer}$$

$$I \propto |E|^2 \propto |F_c|^2 \frac{\sin^2(N_1 \pi H)}{\sin^2(\pi H)} \frac{\sin^2(N_2 \pi K)}{\sin^2(\pi K)} \frac{\sin^2(N_3 \pi L)}{\sin^2(\pi L)} \rightarrow |F_c|^2 N_1^2 N_2^2 N_3^2$$

For (HKL) → integer

Slit interference function

$$S_3(L) = \sum_{-(N_3-1)/2}^{(N_3-1)/2} e^{i\,2\pi\, n_3 L} = \frac{\sin(N_3 \pi L)}{\sin(\pi L)} \rightarrow N_3 \text{ as } L \rightarrow \text{integer}$$

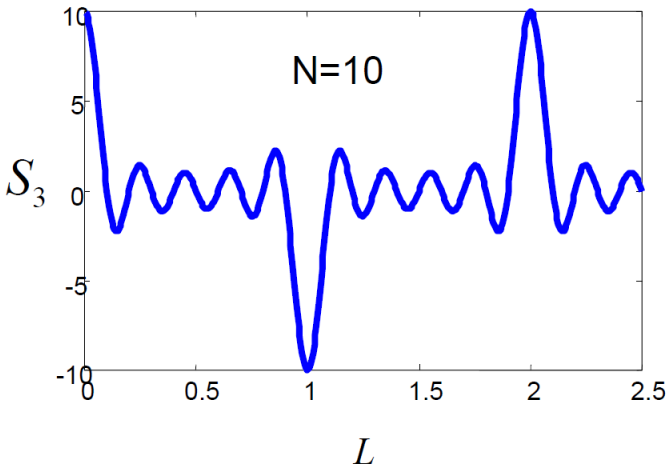

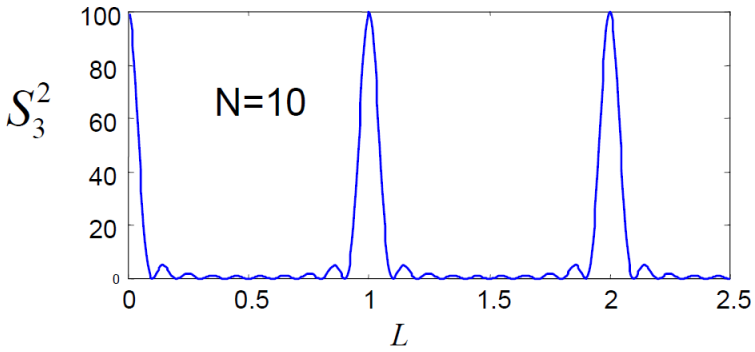

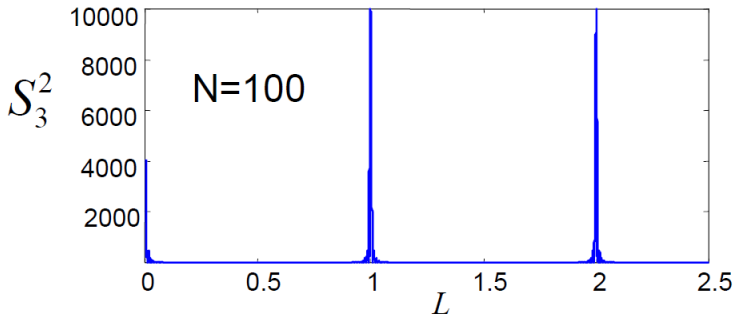

Intensity is nominal for non-integer values. But its not zero if the xtal is finite size!

Lattice factor for terminated surface

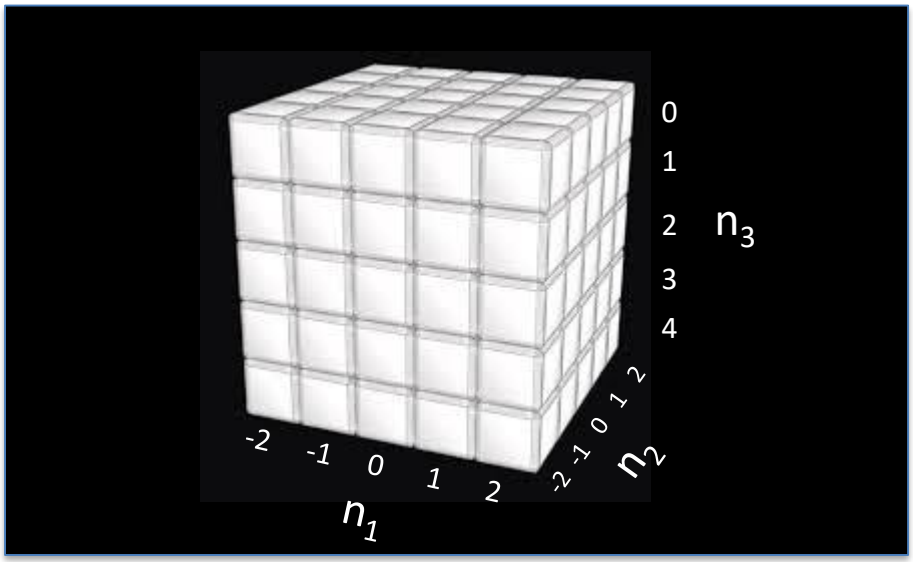

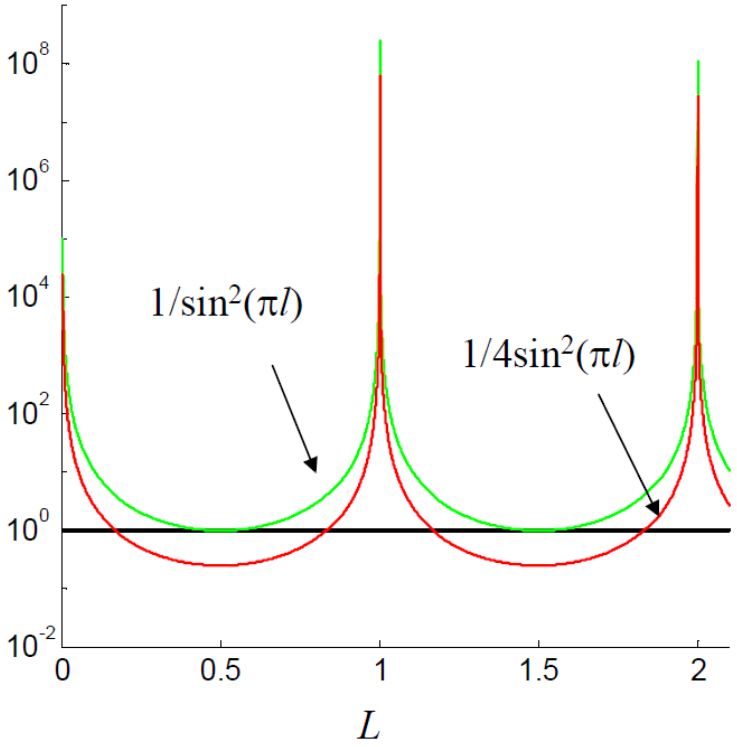

$$E \propto F_c \sum_{-(N_1-1)/2}^{(N_1-1)/2} e^{i\,2\pi\, n_1 H} \sum_{-(N_2-1)/2}^{(N_2-1)/2} e^{i\,2\pi\, n_2 K} \sum_{-\infty}^{0} e^{i\,2\pi\, n_3 L}$$

$$Fctr = \sum_{-\infty}^{0} e^{i\,2\pi\, n_3 L} = \frac{1}{(1 - e^{-i\,2\pi\, L})}$$

$$I \propto N_1^2 N_2^2 \left|F_c(HKL)\right|^2 \left|F_{CTR}(L)\right|^2$$

$$\left|Fctr\right|^2 = \frac{1}{4\sin^2(\pi L)}$$

The crystal truncation rod (CTR) intensity

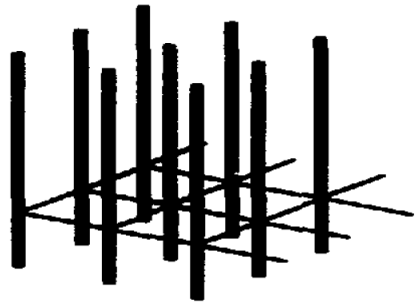

2D LAYER ONLY

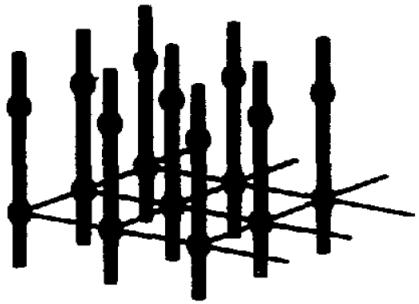

BULK CRYSTAL AND 2D LAYER

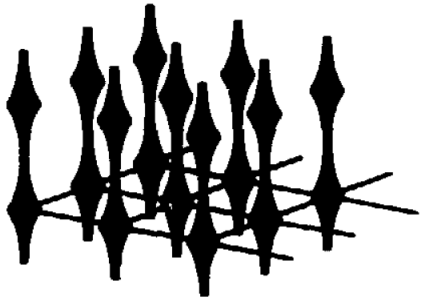

CRYSTAL TRUNCATION RODS

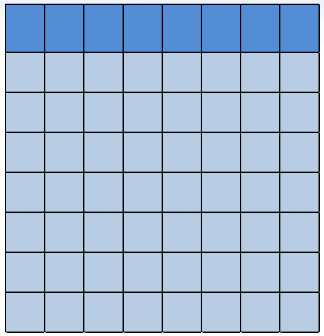

Surface Unit Cells

Bulk Unit Cells

$$E_T = E_{bulk} + E_{surf}$$

$$E_{bulk} = N_1 N_2 \, F_{c,\,bulk}(HKL)\, F_{CTR}(L)$$

$$E_{surf} = N_1 N_2 \, F_{c,\,surf}(HKL)\, e^{i2\pi L}$$

$$I \propto N_1^2 N_2^2 \left| F_{bulk,c} F_{CTR}(L) + F_{surf,c} \right|^2$$

$$F_c = \sum_{j=1}^{n} f_j e^{i\,\mathbf{Q}\bullet\mathbf{r}_j} e^{-M_j} \qquad \mathbf{Q}\bullet\mathbf{r}_j(xyz) = 2\pi(x\,H + y\,K + z\,L)$$

CTR intensity profile provides exquisite sensitivity

- Observe several orders of magnitude intensity variation with changes in surface:
  - atomic site occupancy
  - relaxation (position)
  - presence of adatoms
  - roughness

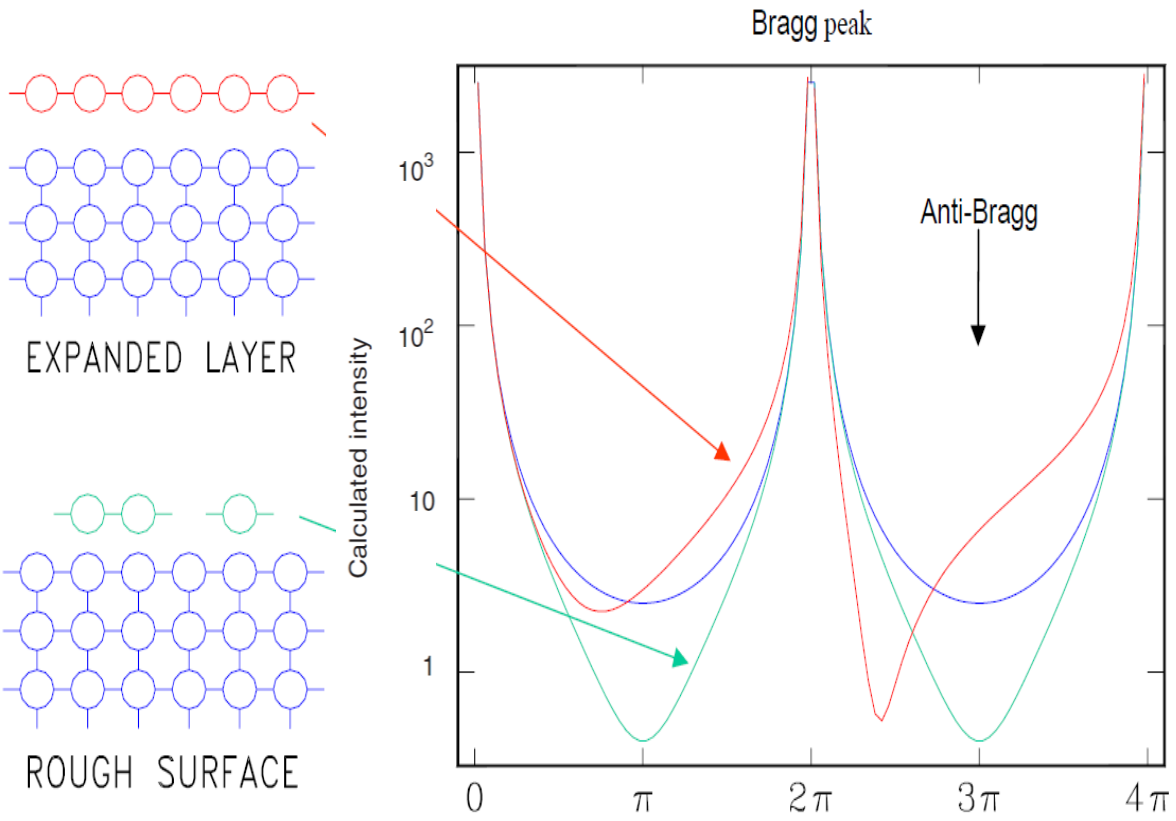

X-Ray Techniques – Crystal Truncation Rods (CTR)

- Crystal Truncation Rod intensity profile is incredibly sensitive to top layer conditions (position, composition, width, etc…)

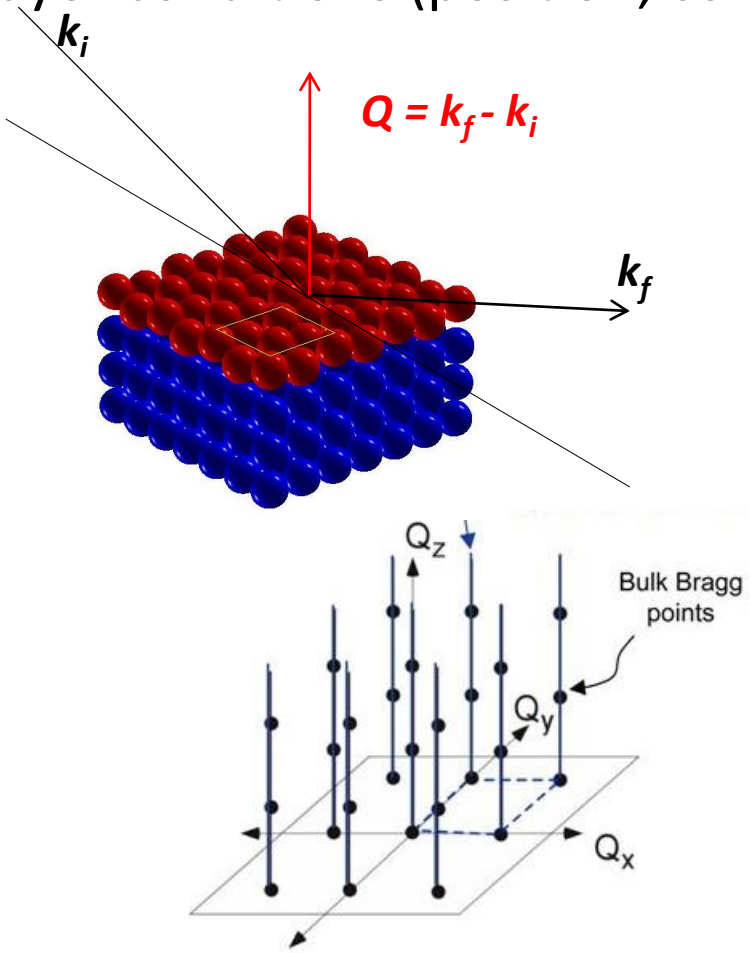

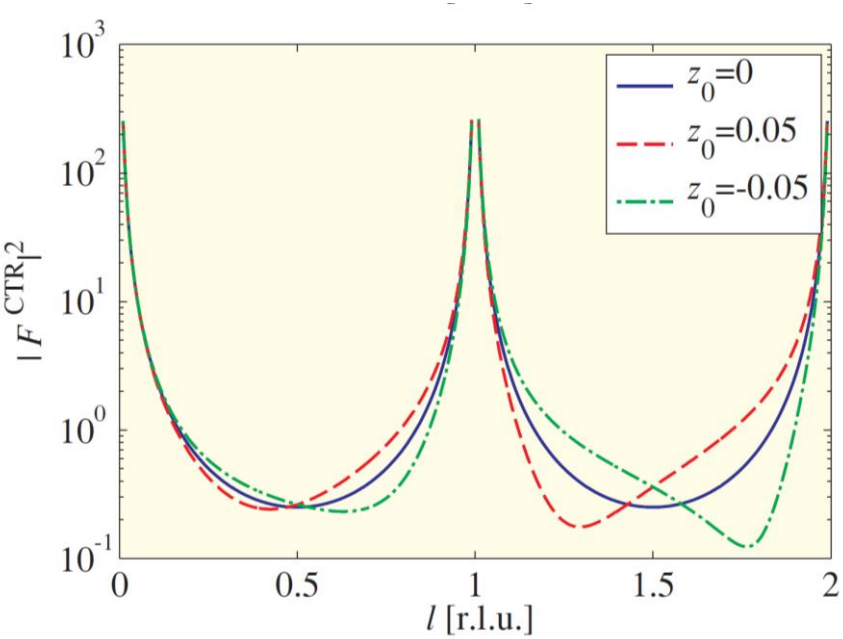

Elements of Modern X-ray Physics
Jens Als-Nielsen, Des McMorrow,
Fig 4.17

CTR analysis applied to water – electrode interface

- Findings show water molecules ordered for about 3 molecular diameters from the electrode
- Spacing for the first layer shows oxygen up (down) average orientation for negative (positive) charge.
- First layer has greater density than bulk water implying the disruption of hydrogen bonding at the interface

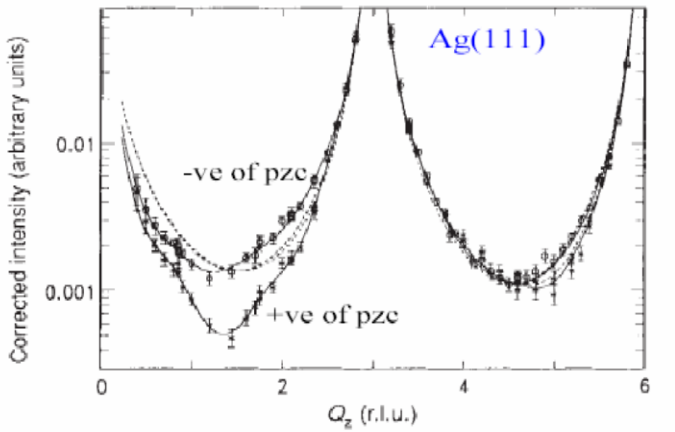

Toney et al., Nature **368**, 444 (1994)

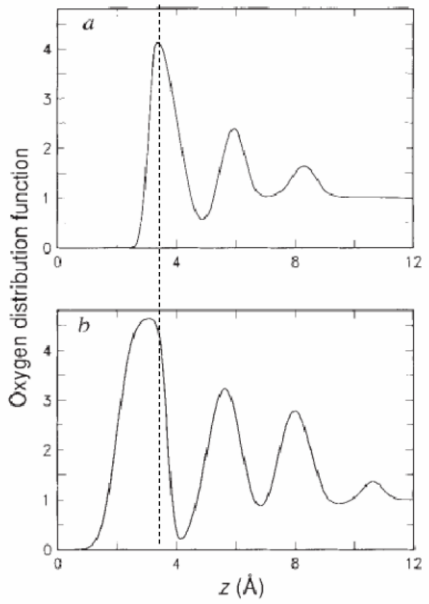

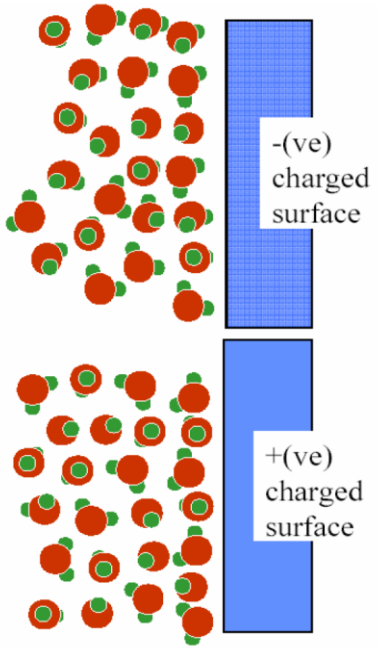

Anomalous scattering contrast

Structure factor of the unit cell

$$F_c = \sum_{j=1}^{m} f_{a,j} e^{i\mathbf{Q}\cdot\mathbf{r}_j} e^{-M_j}$$

$$f(q,E) = f_o(q) + f'(E) + if''(E)$$

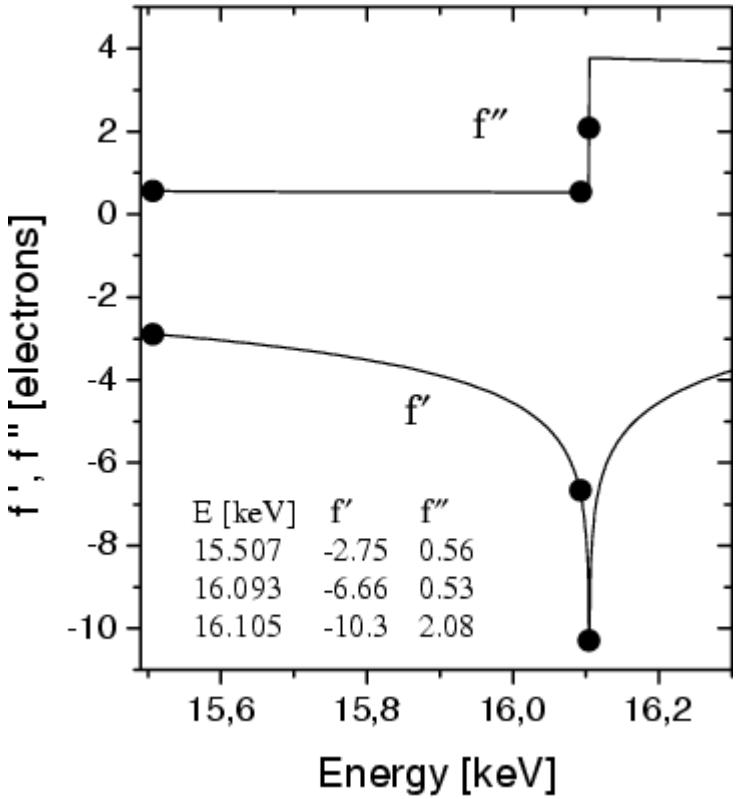

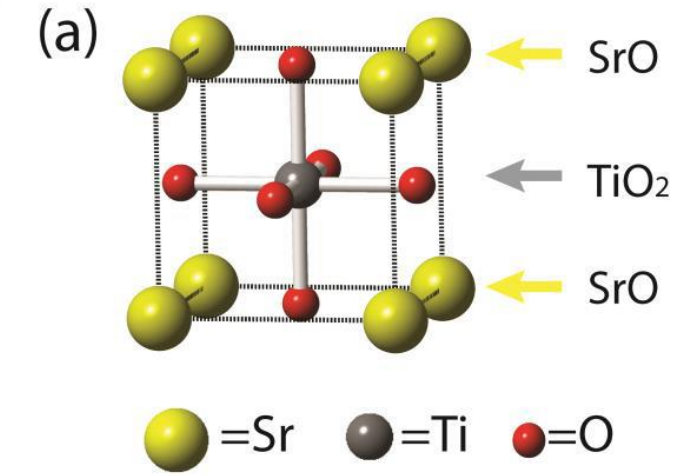

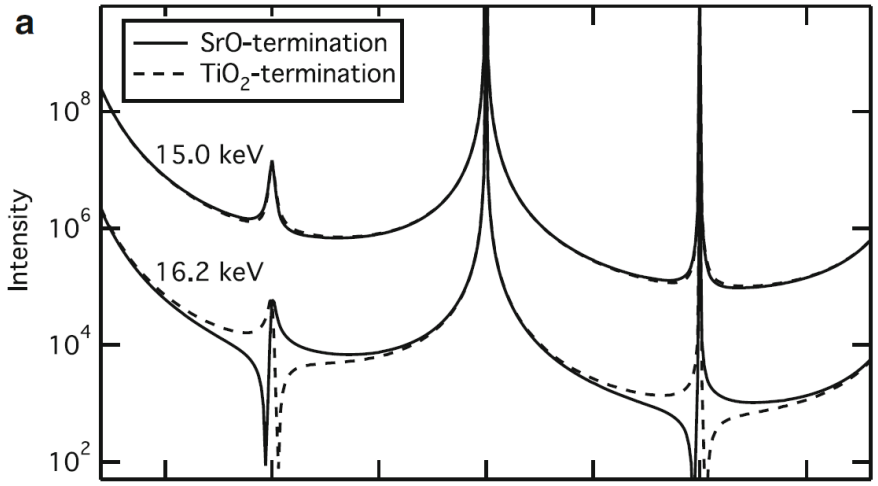

Tim T. Fister and Dillon D. Fong. Thin Film Metal-Oxides: Fundamentals and Applications in Electronics and Energy, Shriram Ramanathan Ed.

Anomalous scattering energy scans at fixed q

- Simulation of Sr in solution near a quartz interface
- Method used to determine model-independent structures

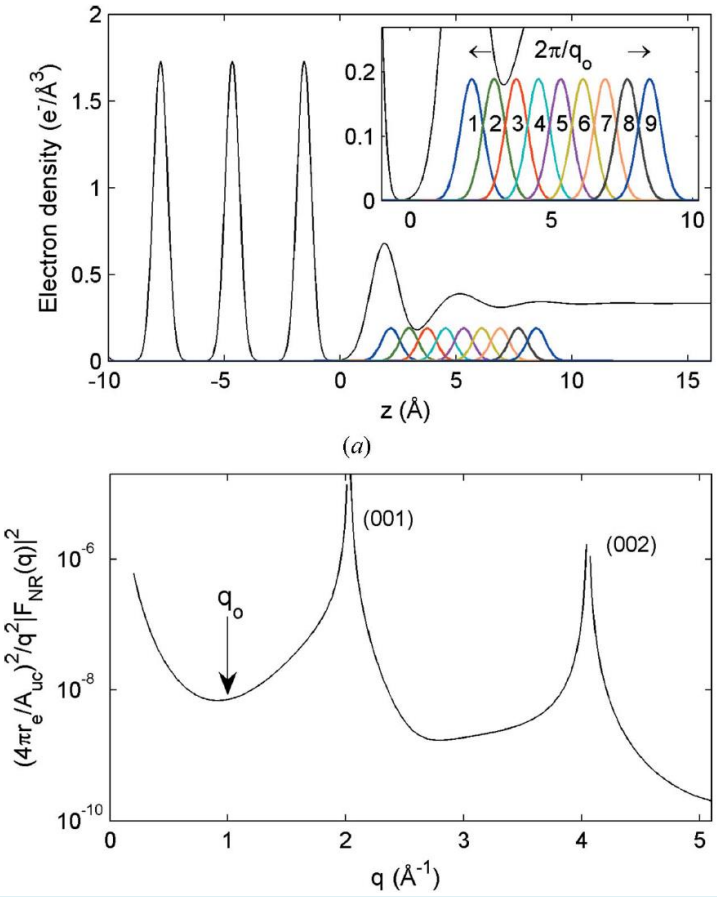

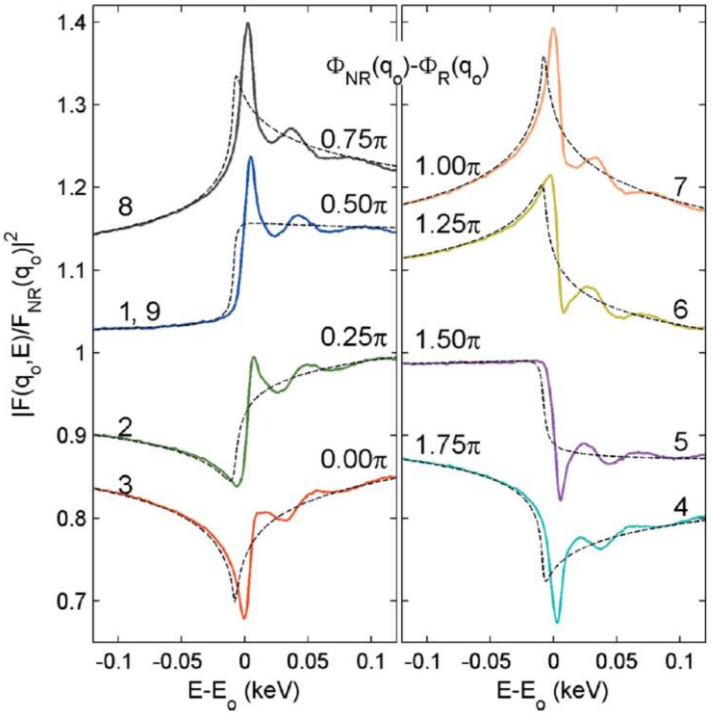

Park & Fenter, *J. Appl. Cryst*. (2007). **40**, 290–301

Interfacial chemistry – cation adsorption

- Scattering near an absorption edge provides elemental sensitivity
- Model-independent elemental distributions determined from the resonant reflectivity data
- Adsorption involves distinct species controlled by the cation hydration enthalpy

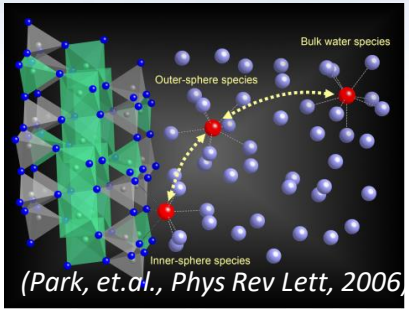

Cation adsorption at the muscovite-electrolyte interface

R(q) reveals the total interfacial density profile

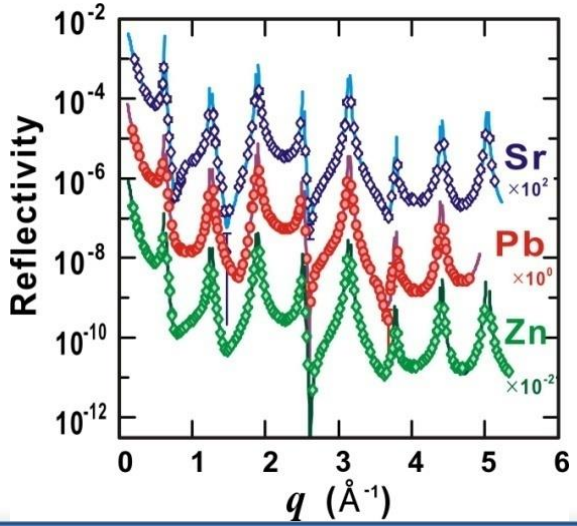

R(E) reveals *the* element-specific density profile

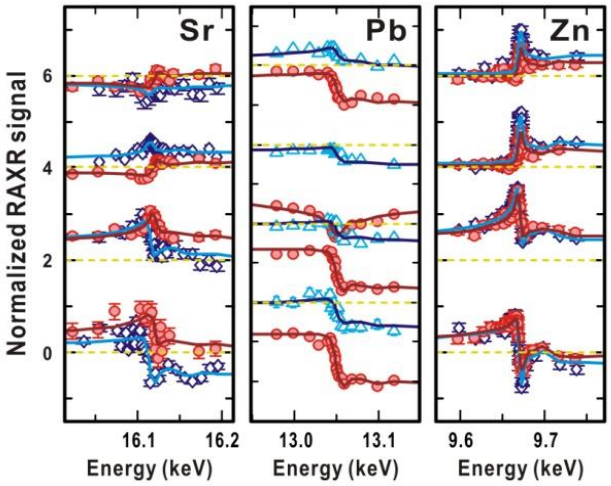

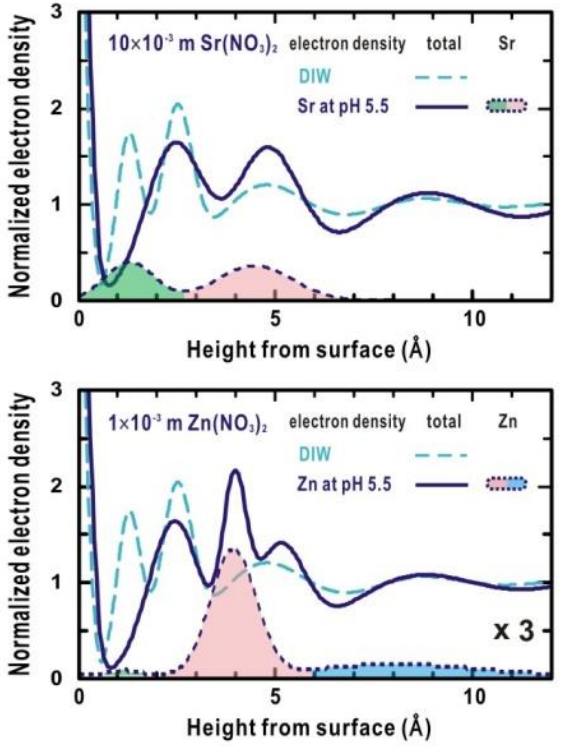

Surface-mediated formation of Pu nanoparticles

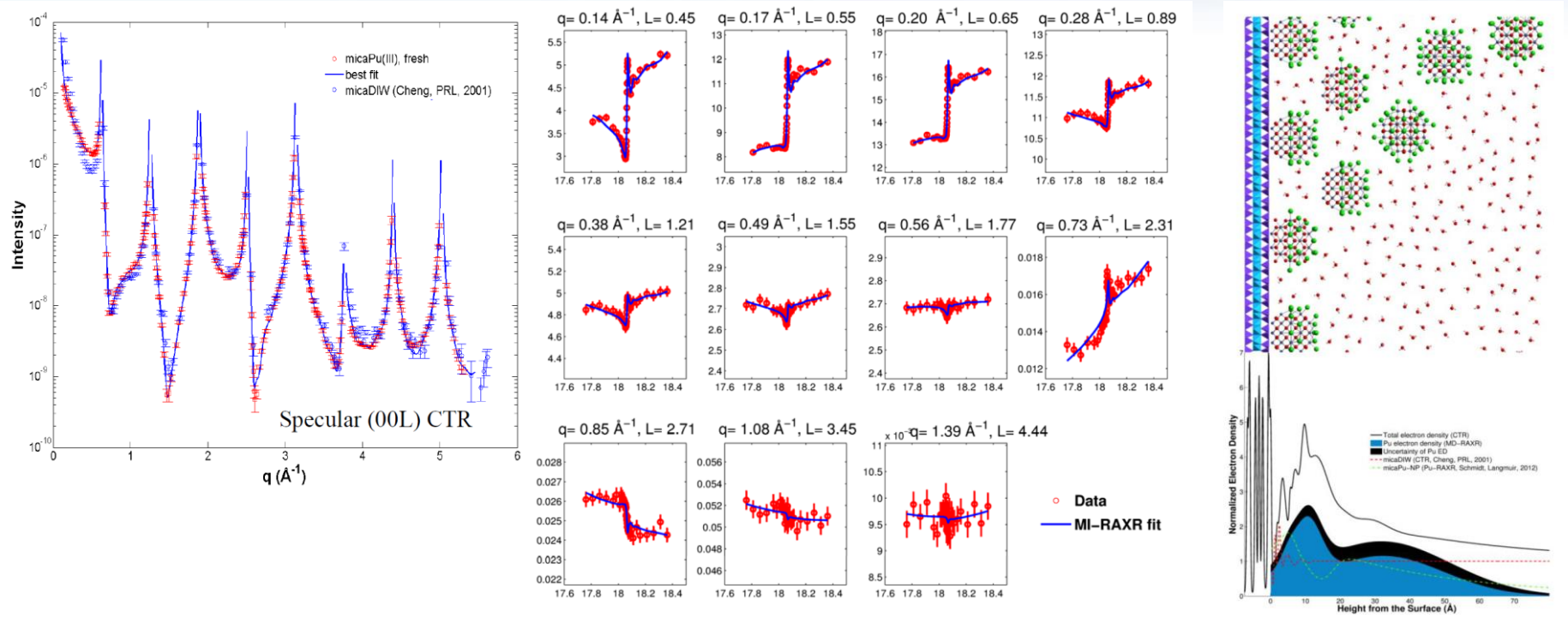

- Pu has broad vertical distribution, peaked at 10.5 Å and extends >70 Å
- Total plutonium coverage >9 Pu/muscovite unit cell (0.77µg Pu/cm²)
- This type of information can inform remediation strategies

M. Schmidt, et al. *ES&T* **47**(24) 14178-14184 (2013)

Scattering/diffraction from high quality films

- Diffraction scattering from thin films can be rather complex
- Strained films diffract to different reciprocal space locations
- Thin film diffraction peaks are broadened along ‘z’
- Reconstructions produce superlattices with different periodicity
- Surfaces that are miscut from the lattice produce tilted crystal truncation rods

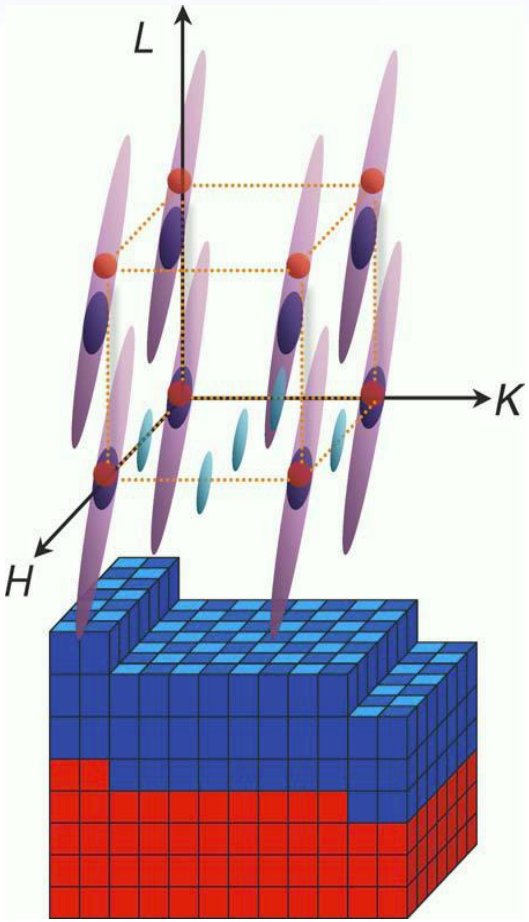

Fong and Thompson, *Annu. Rev. Mater. Res*. (2006)

CTR data collection

- Area detectors allow efficient collection of CTR data
- Generally, CTRs are rotated through the Ewald sphere to probe different parts of the rod
- Specular rods provide access to information concerning conditions normal to the surface only
- Non-specular CTRs provide information about lateral registry too

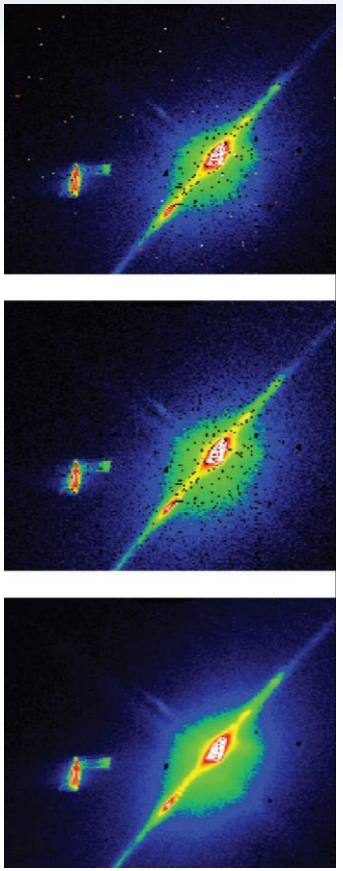

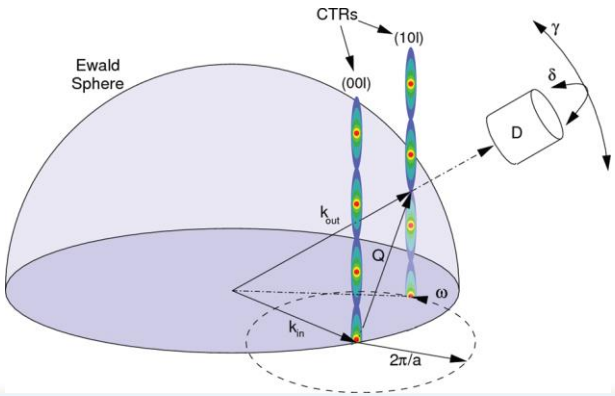

Transistor gate length reduction

Semiconductor Foundry Market: $48.8B in 2015

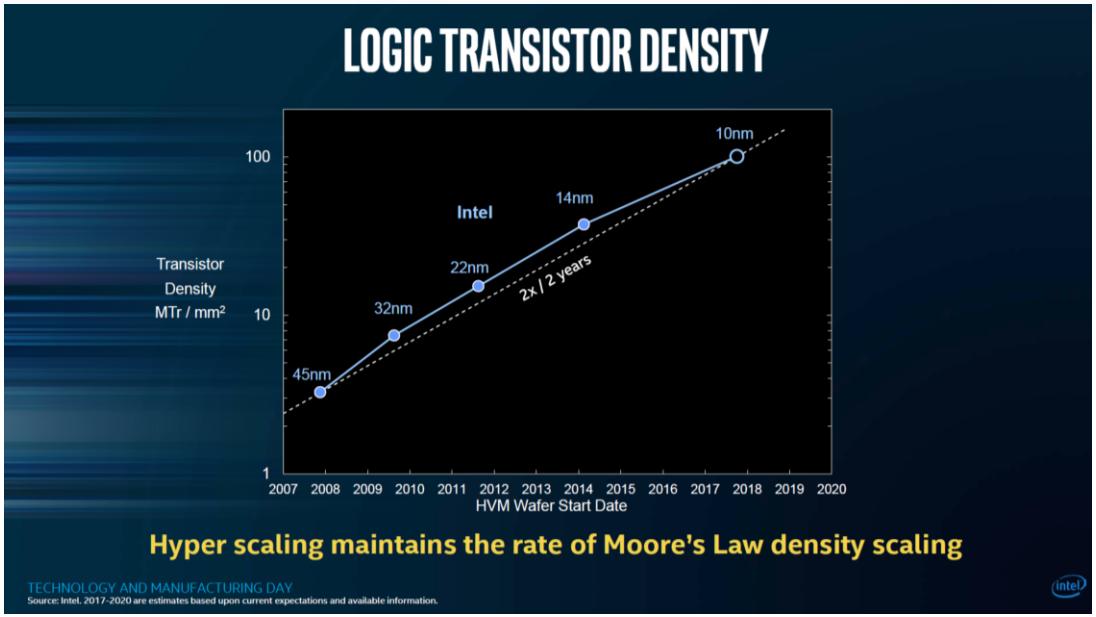

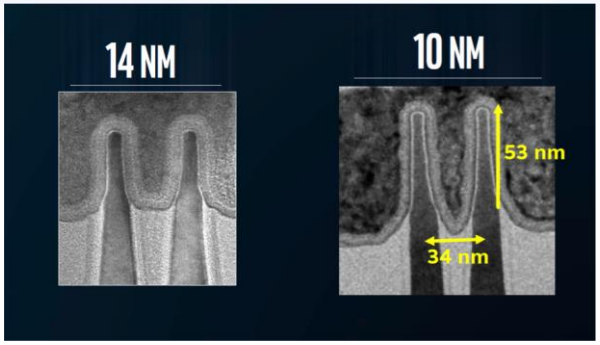

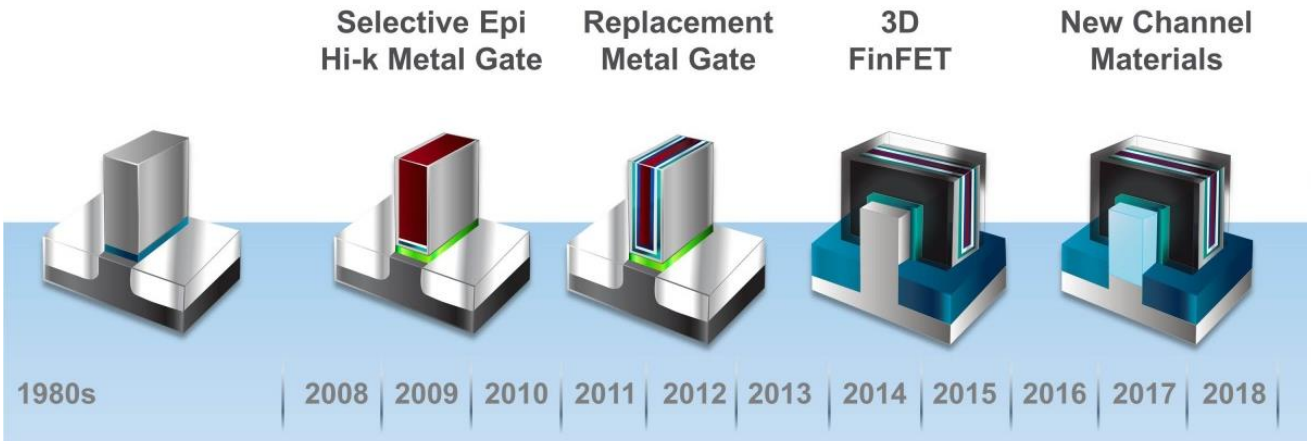

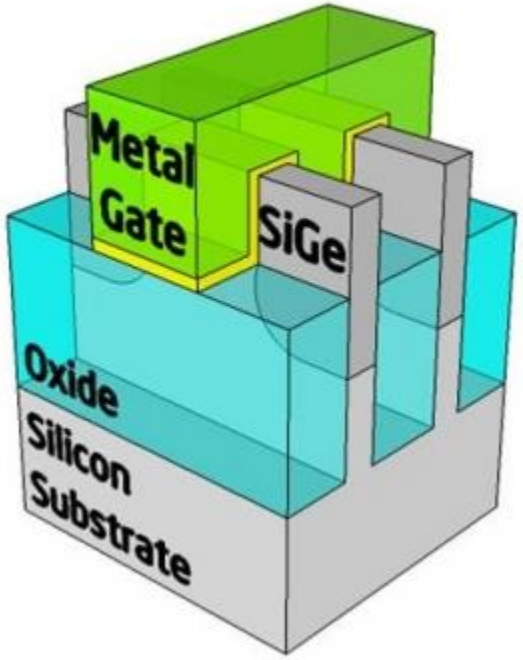

Materials growth

- Vapor phase epitaxy
- Liquid phase epitaxy
- Molecular beam epitaxy
- Sputtering
- Evaporation
- Pulsed laser deposition
- Atomic layer deposition
- Chemical vapor deposition

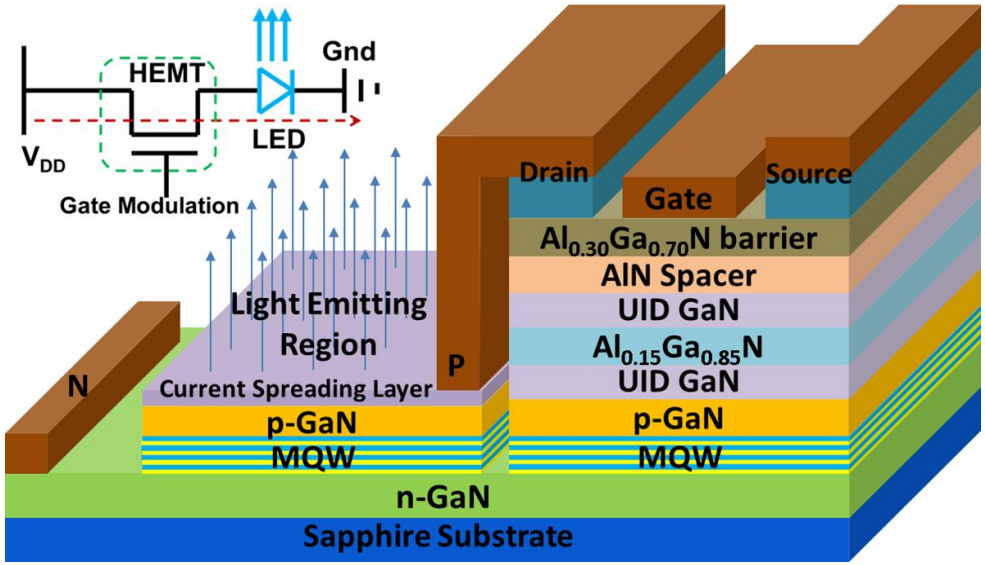

http://www.ece.ust.hk/~ptc/research.php

Challenges in materials growth and processing

- Discovery of new materials with new properties and functionality, e.g.
  - Highly efficient lighting
  - New catalysts
  - High performance batteries and fuel cells
- Exciting areas of current interest:
  - complex oxides with emergent properties
  - quantum confined structures
  - Nano-structures
- *In situ* x-ray techniques are powerful tools
  - structure-property relations
  - operating or native conditions
  - materials synthesis
  - etching & dissolution

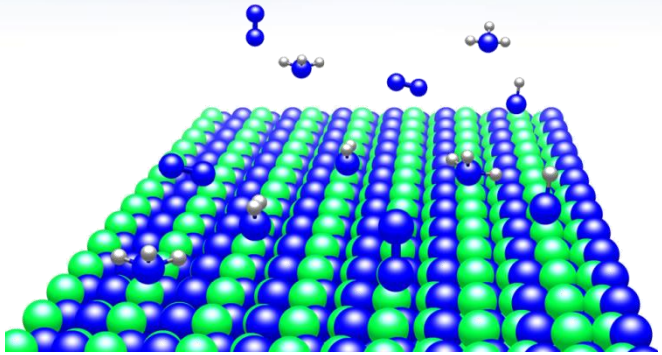

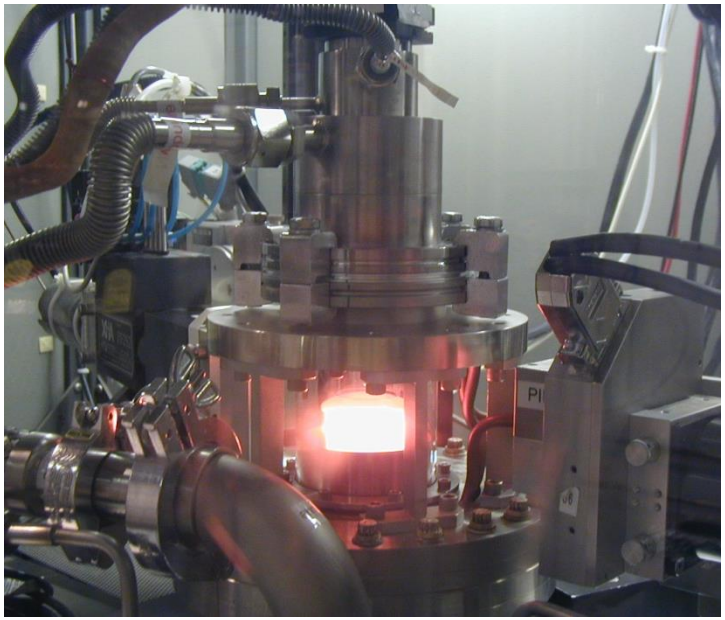

Understanding growth processes & morphology

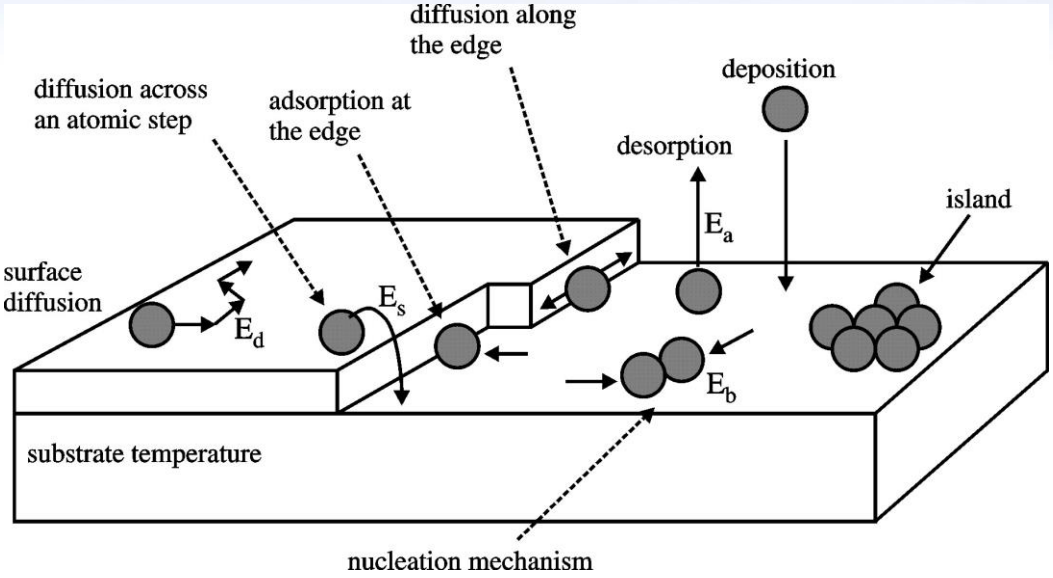

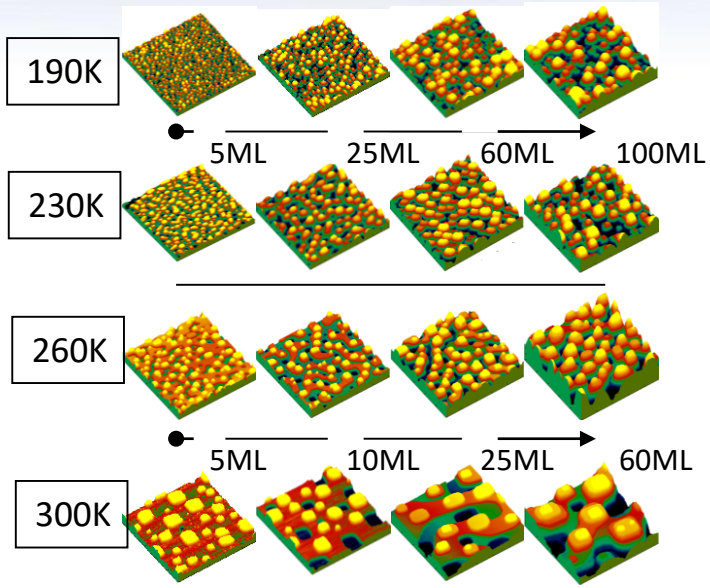

Jim Evans, Iowa State Univ (2005)

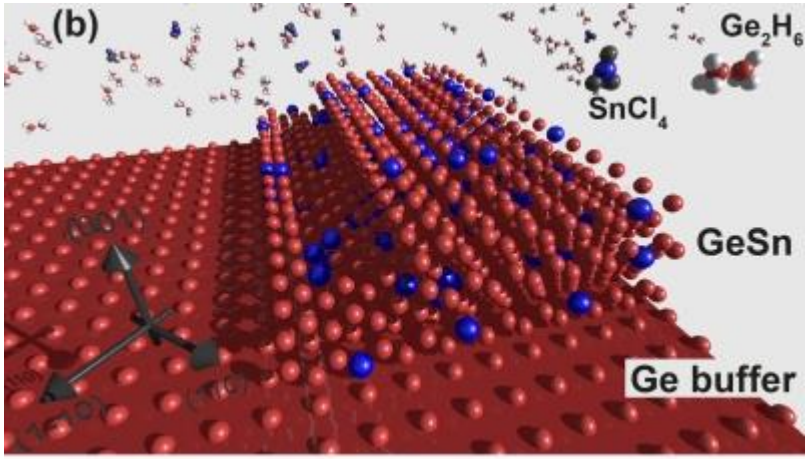

Modeling for Ag on Ag(111)

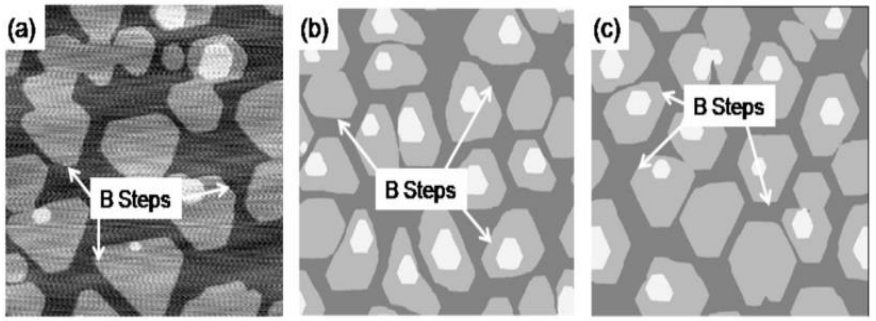

Maozhi Li, et. Al.,Phys. Rev. B, 77, 033402 (2008)

Epitaxial growth modes

- A kinetic Monte Carlo simulation of the main processes that happen during crystal growth in molecular beam epitaxy. (Vladimir Kaganer, 2013)

X-Ray techniques – determination of growth modes

- We can determine growth mode by observation of CTR intensity during growth

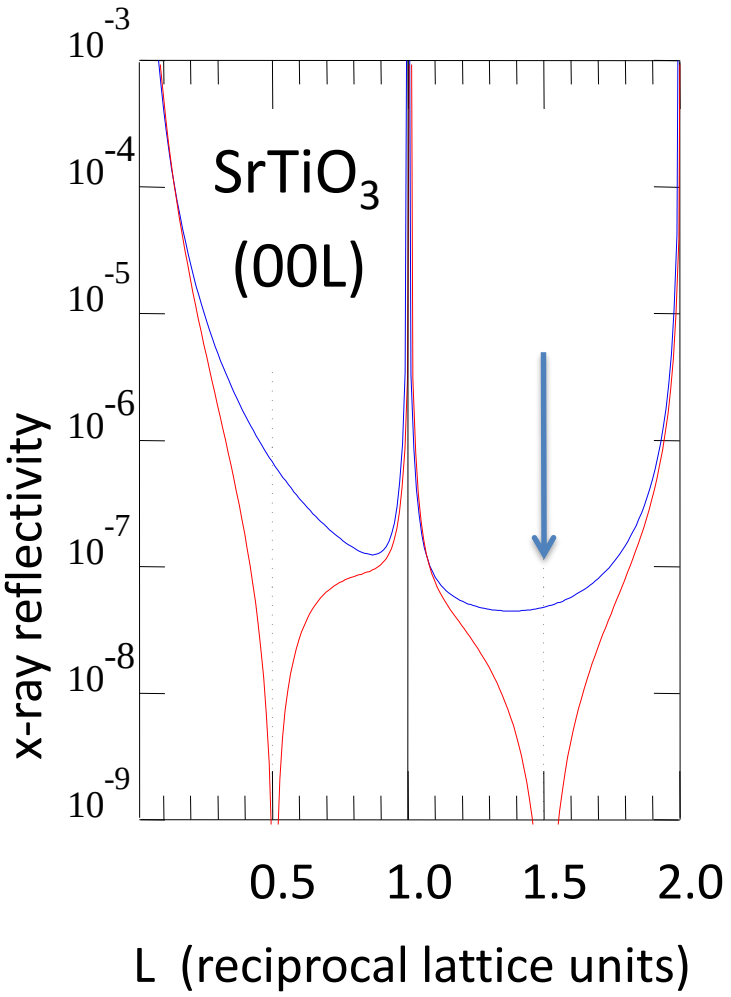

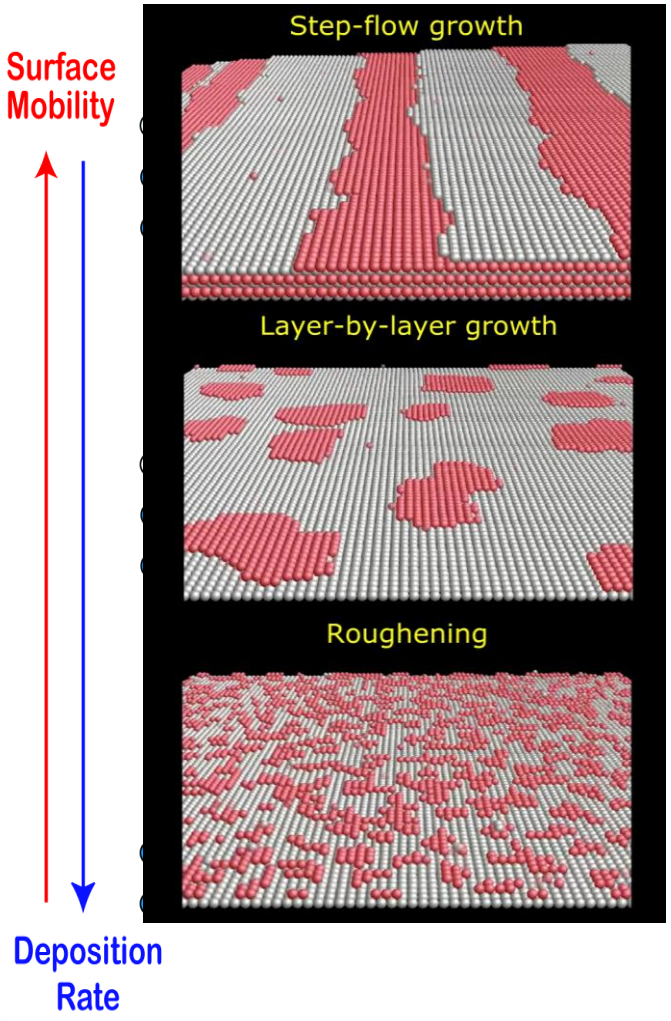

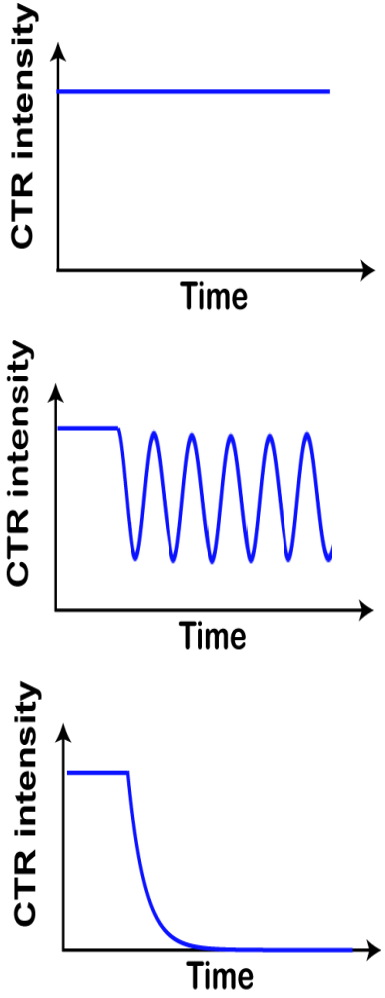

Pulsed-Laser Deposition (PLD)

- The PLD process has a number of characteristics that are fundamentally advantageous for the study of the kinetics of crystal growth far from equilibrium:
- In PLD, the affects of material deposition can be separated in time from surface evolution

PLD consists of periodic bursts of highly driven growth followed by relatively long periods of uninterrupted surface relaxation, permitting these two competing processes to be isolated from each other and studied separately.

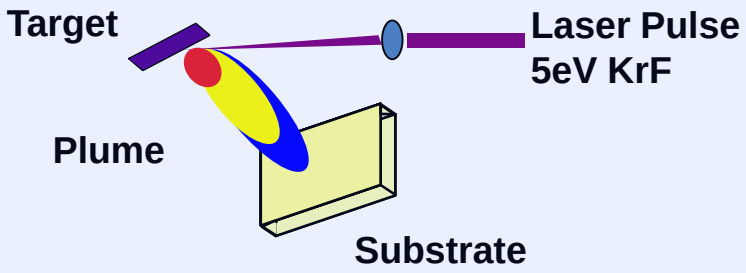

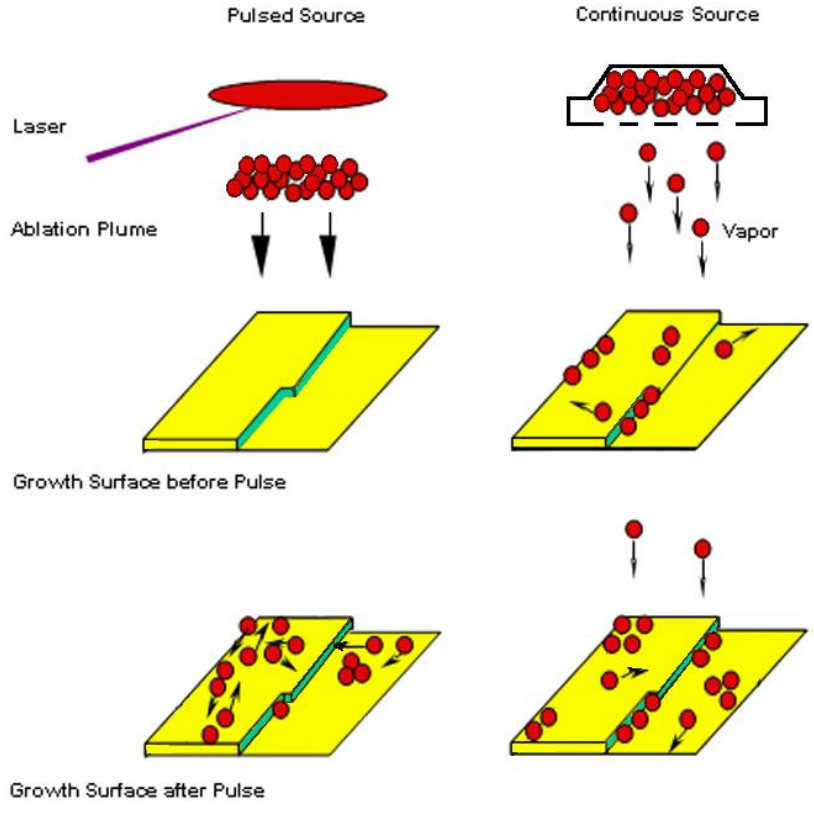

The PLD experimental apparatus

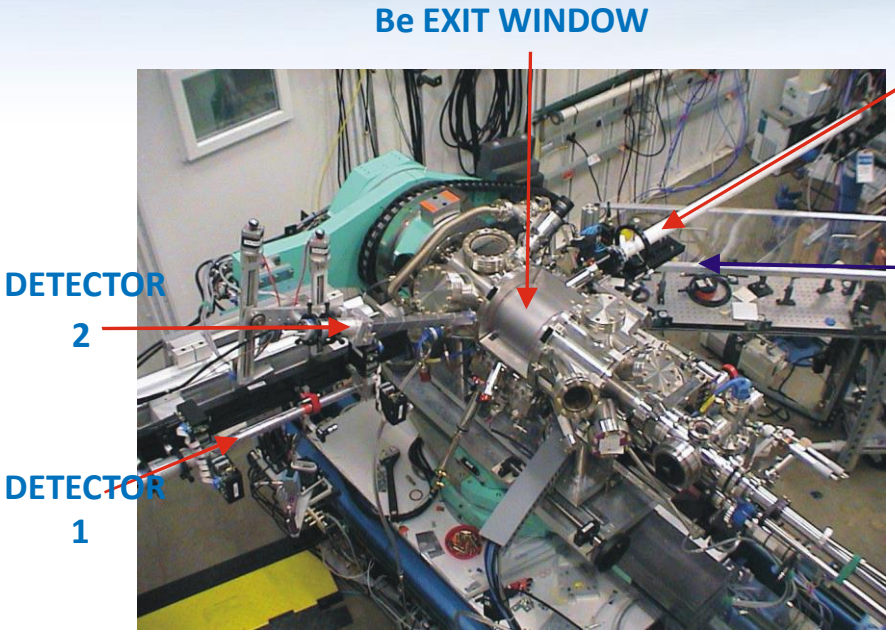

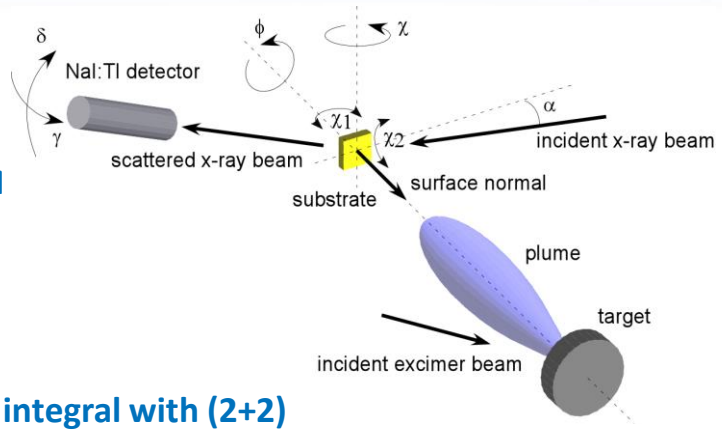

PLD chamber integral with (2+2) diffractometer optimized for surface diffraction.

- Epitaxy with very smooth surfaces at low growth temperature
- Excellent control of growth rate – multilayer and superlattice fabrication
- Simple operation process, low cost and no hazardous precursors required
- Exact stoichiometric transfer of materials from target to substrate - high quality complex films (eg. YBCO)
- Many growth parameters to control (laser parameters, target, substrate, pressure)

Signatures of ideal pulsed growth

- Continuous growth (eg: MBE) vs ideal pulsed growth
- PLD is very similar to ideal pulsed growth

$I=(1-2\theta)^2$

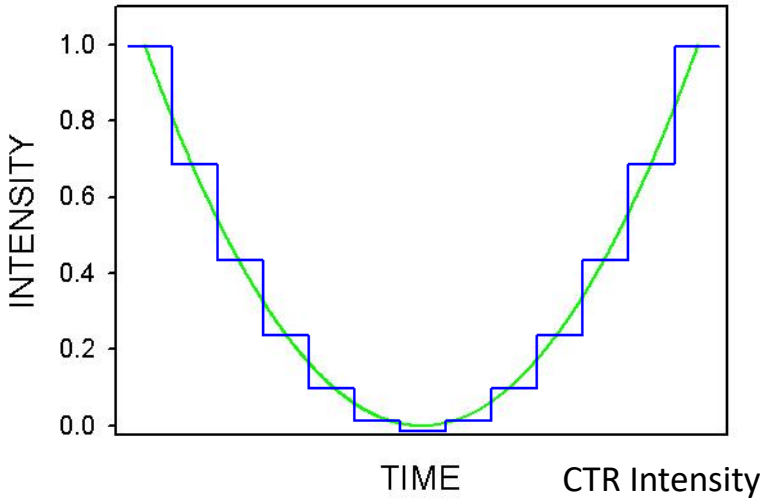

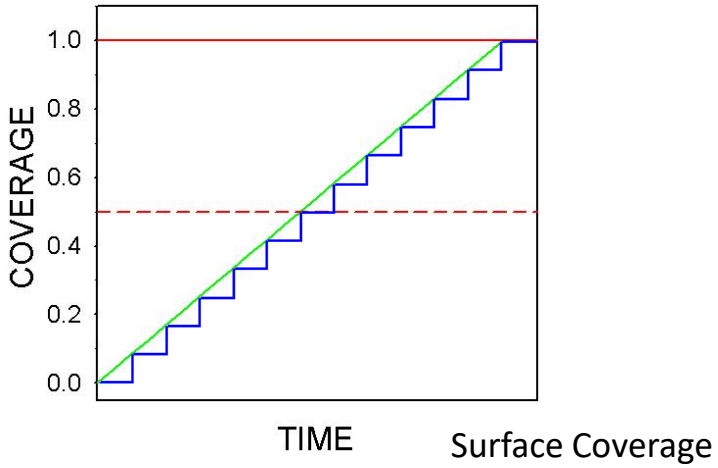

THEORETICAL WORK ADDRESSING PULSED GROWTH:

N. Combe and P. Jensen, PRB **57**,15553 (1998)

B. Hinnemann *et al.* PRL. **87**, 135701 (2001), PRE **67**, 011602 (2003)

CTR oscillations during STO homoepitaxial growth

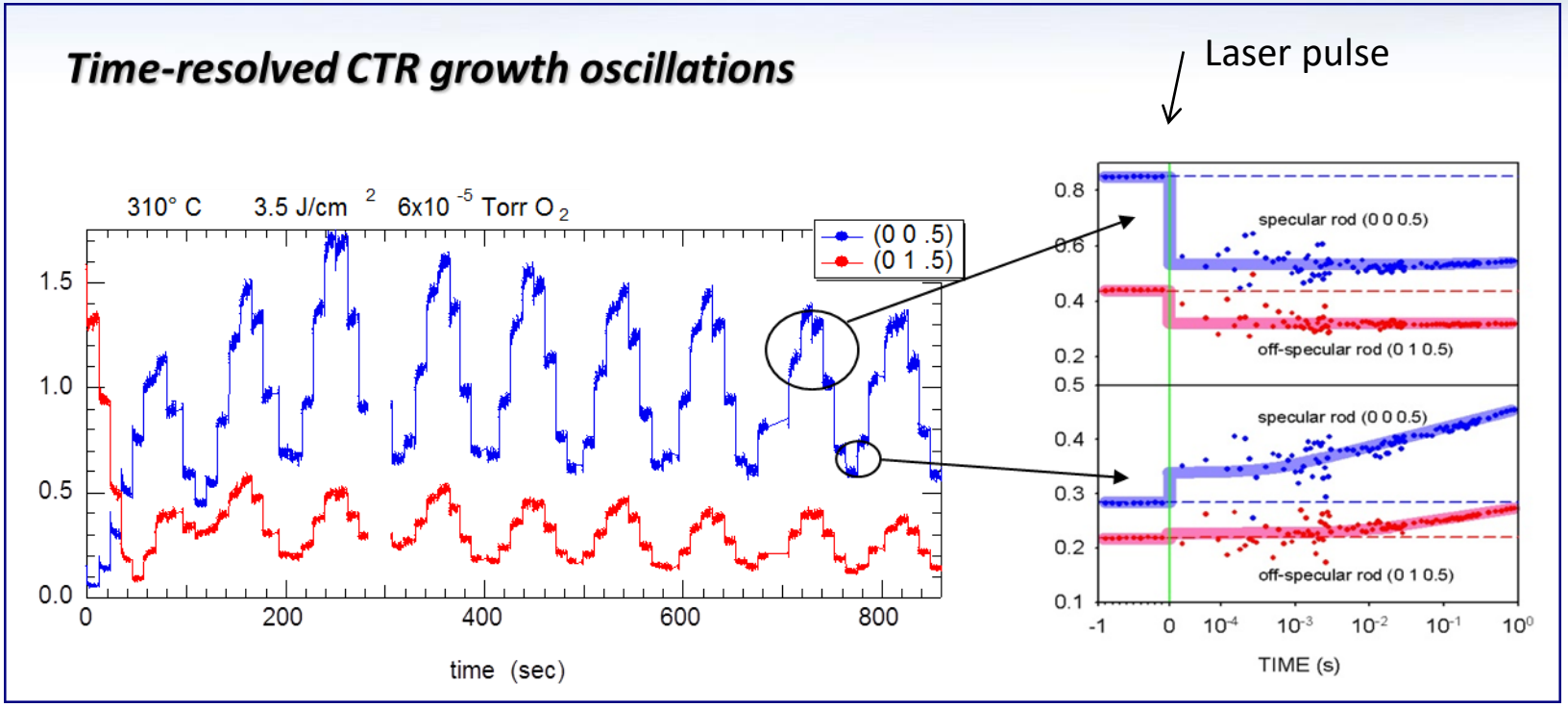

- Abrupt change in specular and off-specular rod intensity occurs simultaneously indicating crystallization occurs concurrently with the arrival of the ablated plume
- Abrupt change occurs faster than current measurement time resolution
- The mechanism of energy enhancement remains elusive and requires further study with improved time resolution – better than current 2-5 msec.

Temperature effect on growth mode

2D Layer Growth – 3D Island Growth

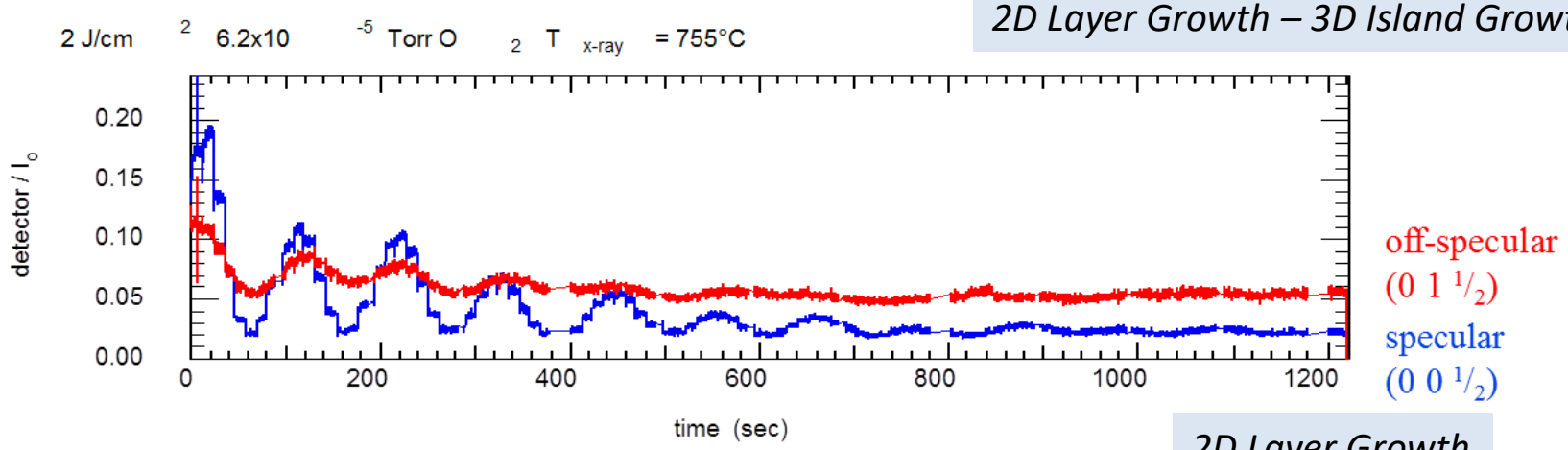

2D Layer Growth

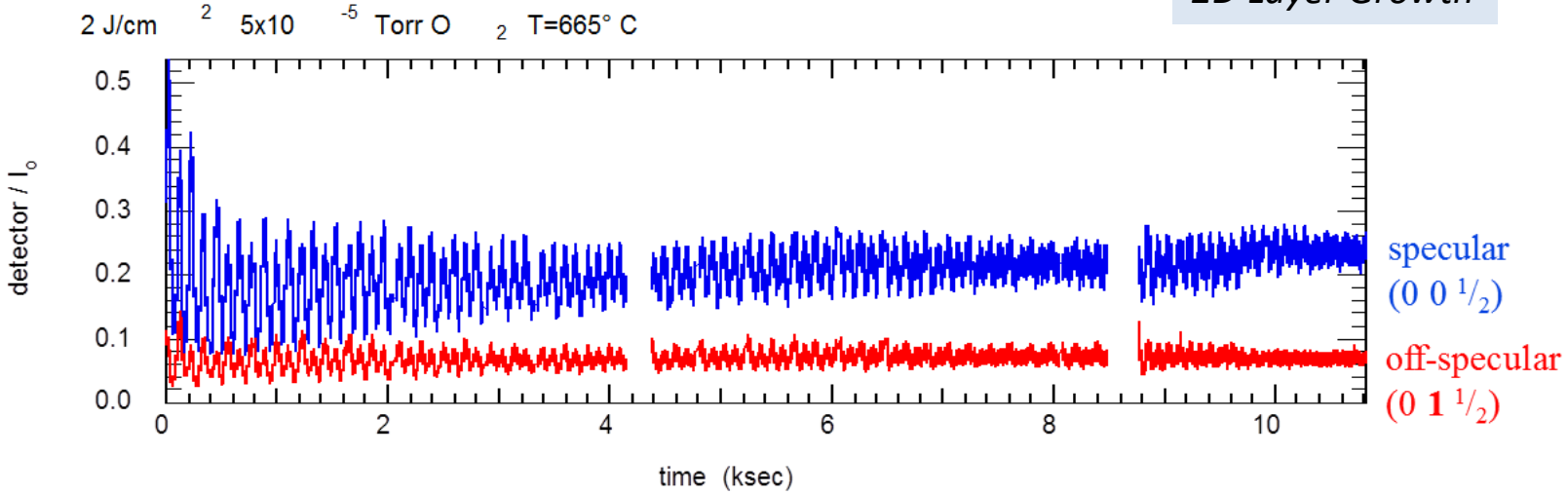

Effect of temperature on in-plane order

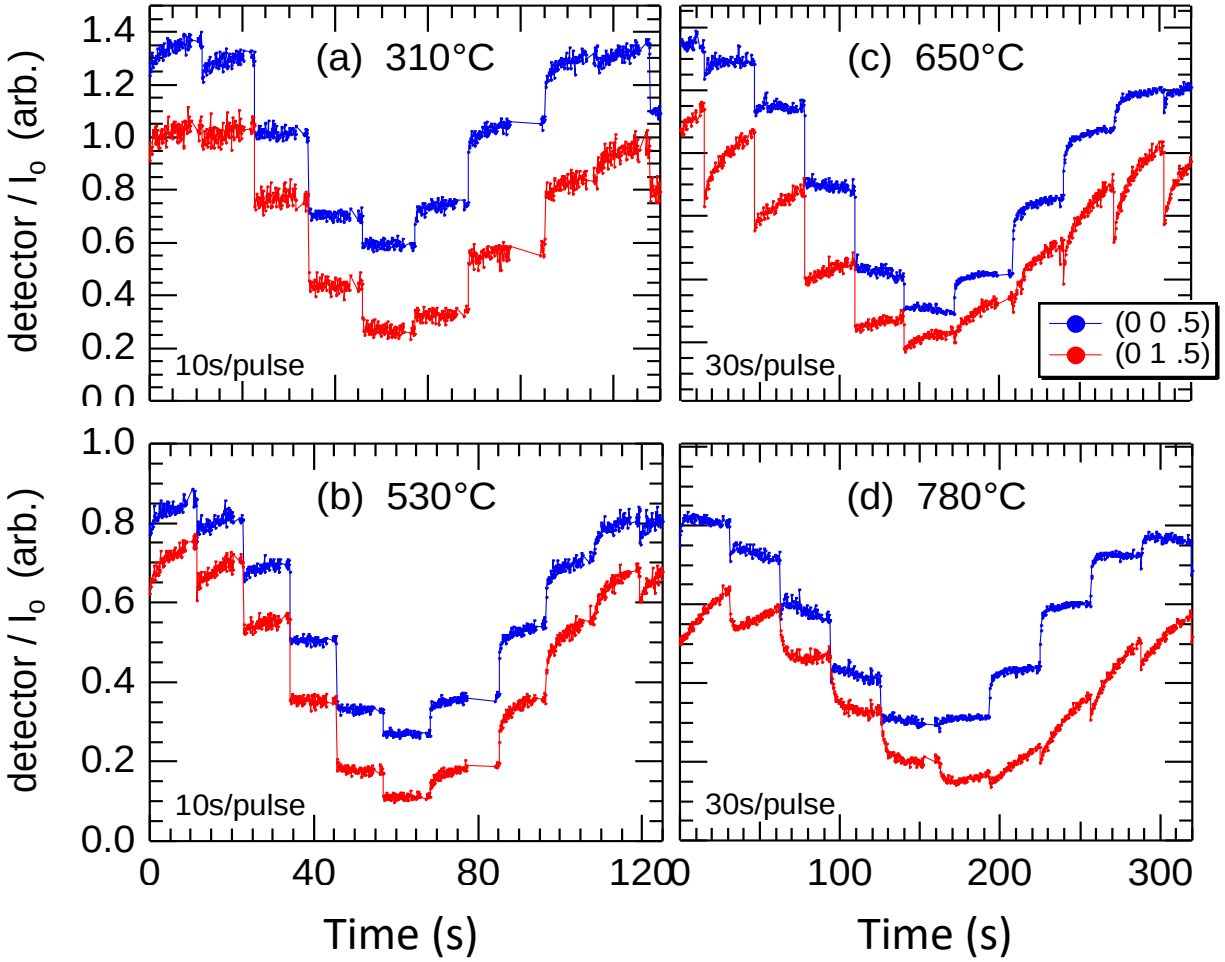

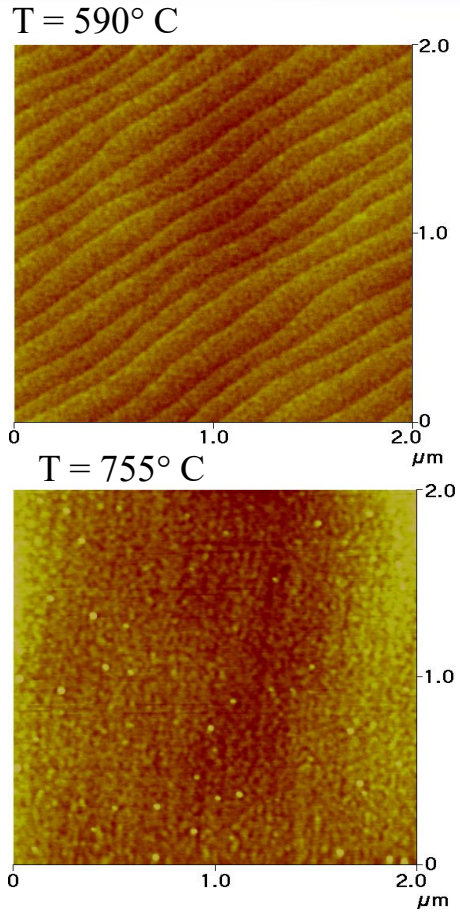

Simple model used for slow decay

- Model does not depend on any specific transport model

Rate ~ (material on level 2) x (area of holes in bottom)

$$\theta_2' = -\frac{\theta_2(t)\theta_0(t)}{\tau}$$

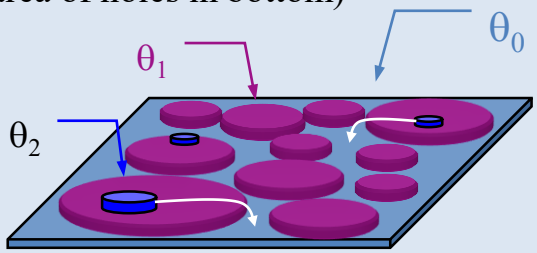

Where $b + \theta_2(t) = \theta_0(t)$ is the area of holes

$$b = 1 - [\theta_2(t) + \theta_1(t)] = 1 - \theta_{total}$$

Solution to diff. eq.

$$\theta_2(t) = \frac{be^{bC}}{e^{bt/\tau} - e^{bC}}$$

Boundary condition

$$C = \frac{\ln\left(\frac{\theta_2(t=0)}{b + \theta_2(t=0)}\right)}{b}$$

Understanding Layer Formation

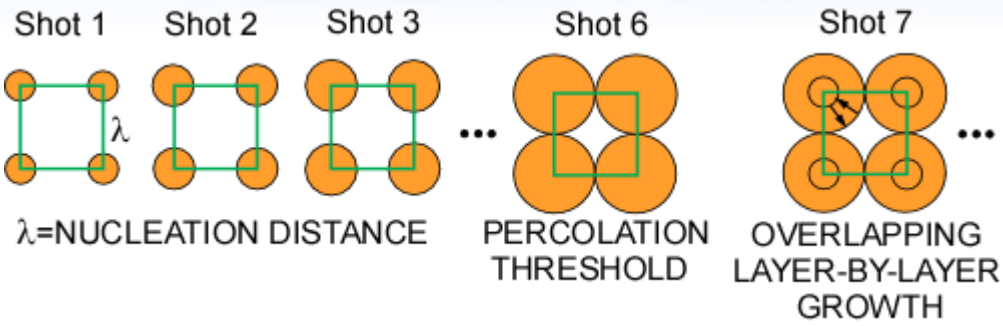

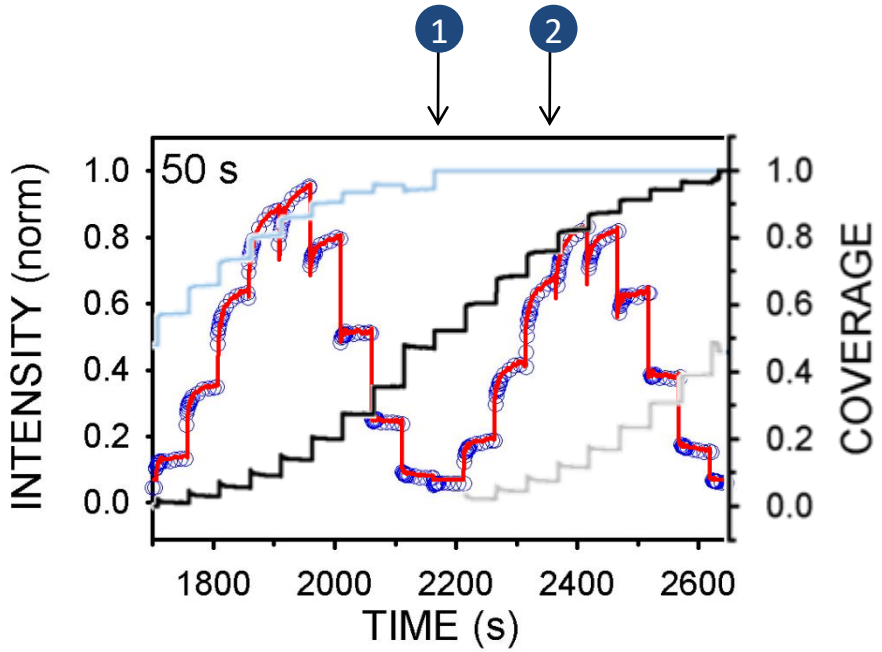

Tischler J. et al. PRL **96**, 226104 (2006)

INSTEAD OF USING TRANSPORT MODELS TO FIT THE DATA WE EXTRACT THE TIME-DEPENDENT COVERAGES DIRECTLY FROM THE SXRD TRANSIENTS USING:

$$I(t)=I_0[(1-2\theta_n(t)+2\theta_{n+1}(t))]^2$$

$\theta_n(t)+\theta_{n+1}(t)$=**DEPOSITION PER PULSE**

THE TIME-DEPENDENT COVERAGES $\theta_n(t)$ **AND** $\theta_{n+1}(t)$ **ARE NOT FLAT!**

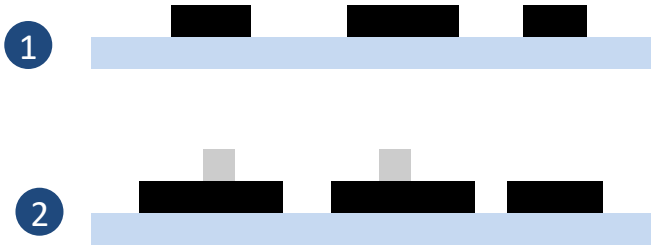

Stable 2-layer growth

A Simple Conventional view

10 shots / layer

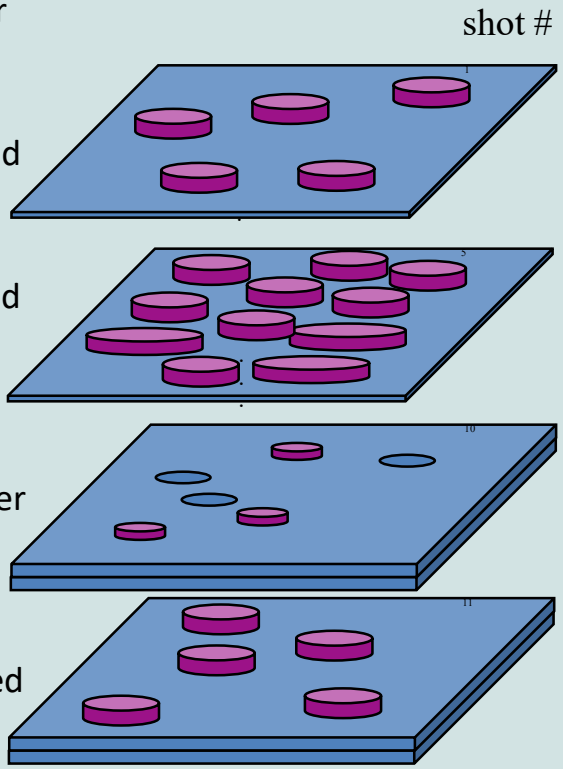

First shot has no interlayer transfer

Rapid Interlayer transfer off half-coverage islands

Sluggish Interlayer transfer due to long random walk, leaving ~5% holes + ~5% islands

Shot 11 fills remaining holes and adds to new layer; Coverage the same as after shot 1.

Since the surface repeats, Growth proceeds without roughening

Self-similar in the time domain

- Dwell time between shots varies by x250, but 5Hz (0.2sec) data still shows rounding similar to 50 sec data (τ is changing). So sizes at 5Hz must be smaller than 50sec

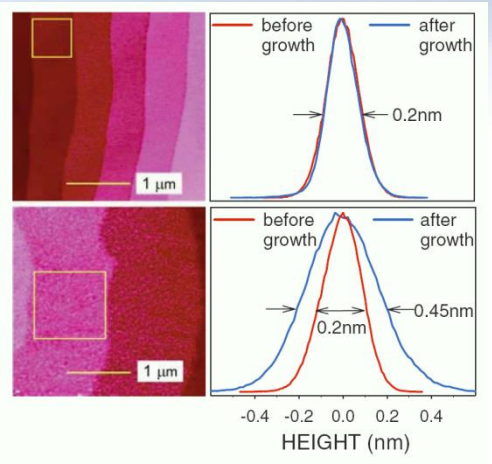

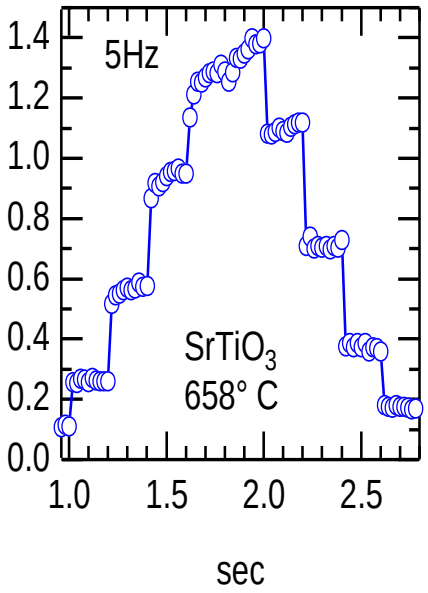

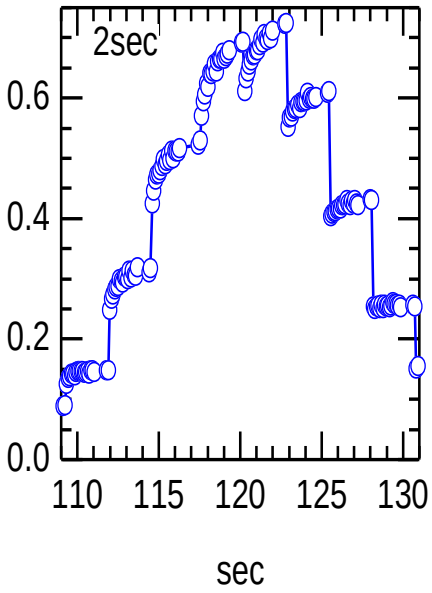

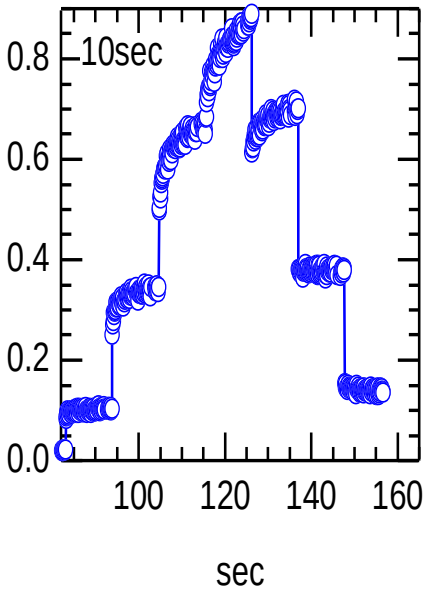

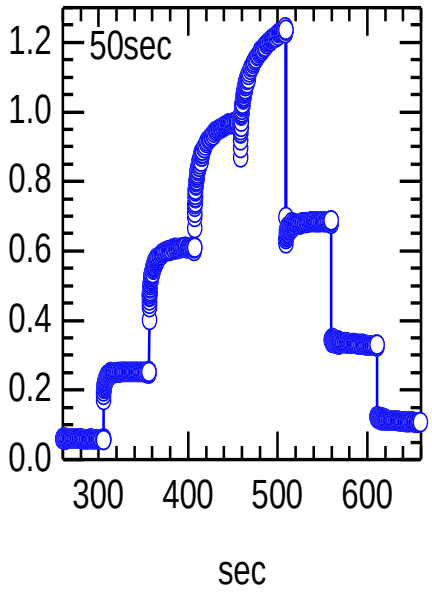

Diffuse surface scattering from Ag during growth

- Diffuse peak position contains correlation distance information
- Diffuse peak width relates to size distribution

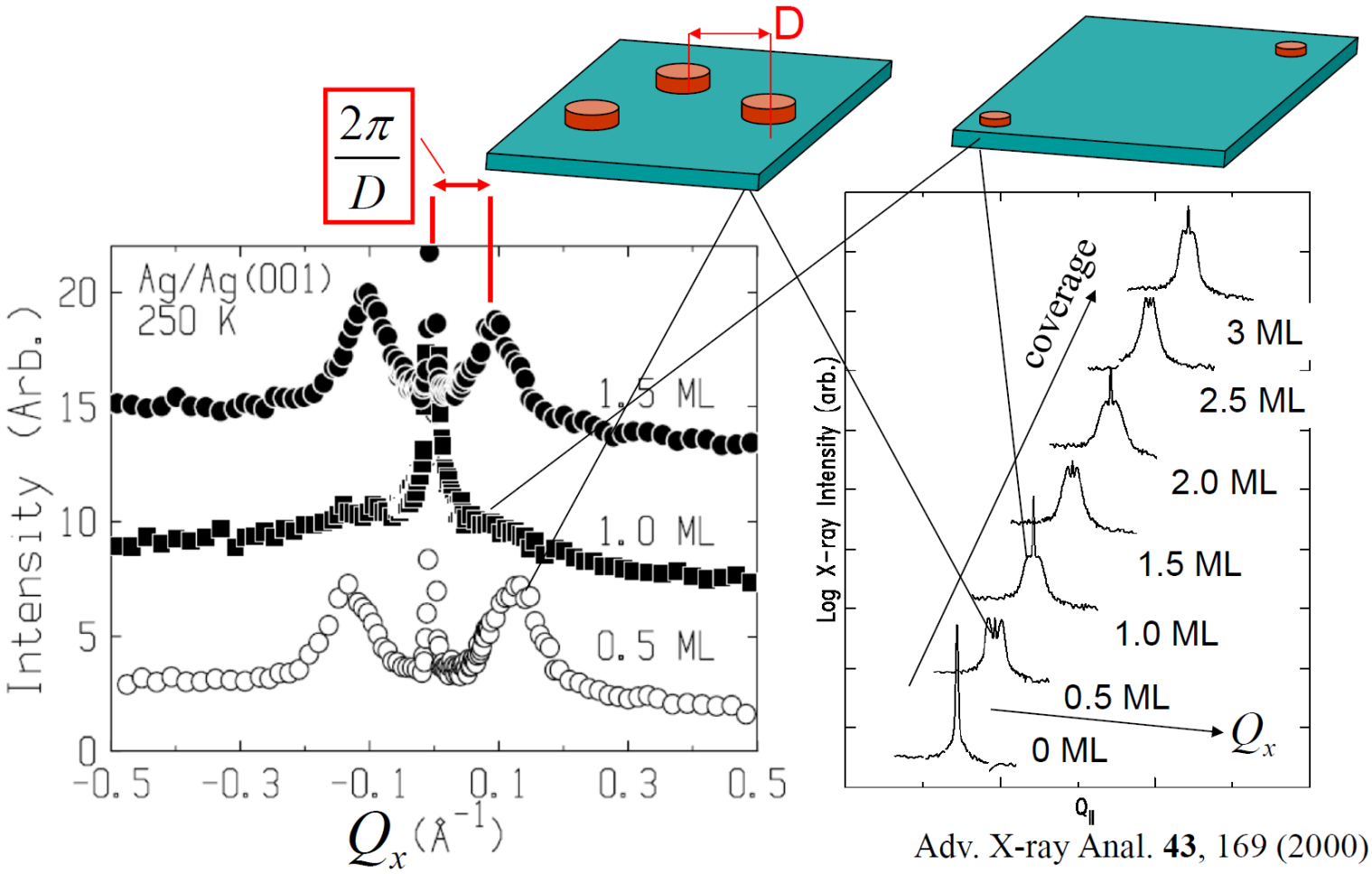

Adv. X-ray Anal. **43**, 169 (2000)

Island size evolution in STO PLD

- The island size and the spatial distribution of islands can be determined from the diffuse scattering component.
  - Diffuse peak position contains correlation distance information
  - Diffuse peak width relates to size and distribution
- Small island regime is at short dwell times and lower temperatures

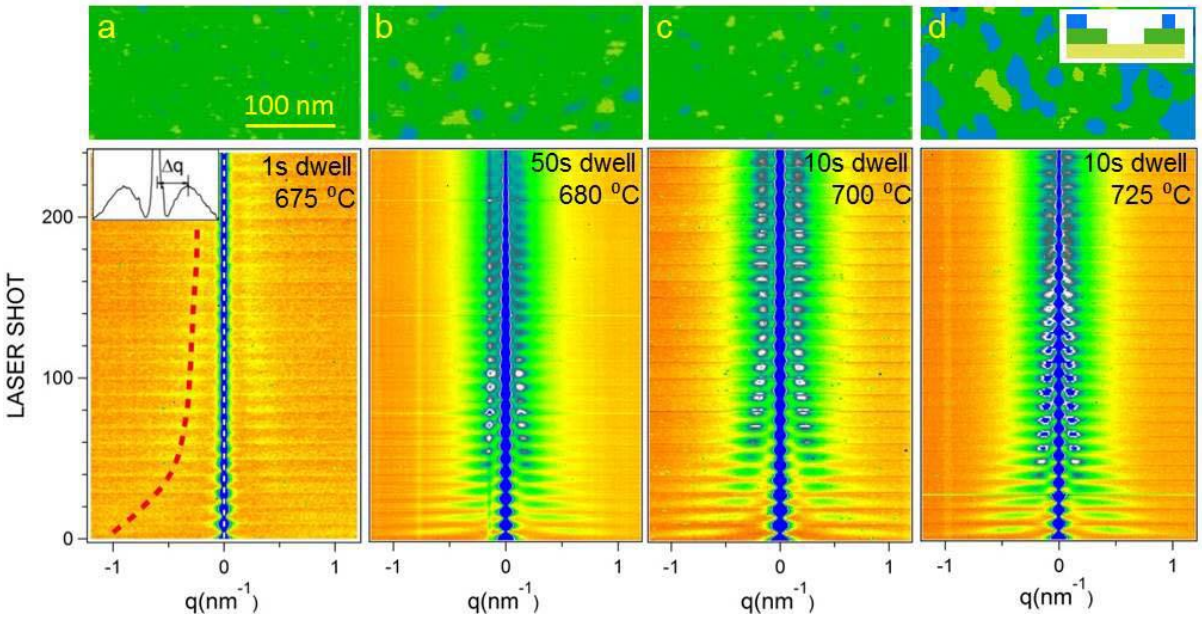

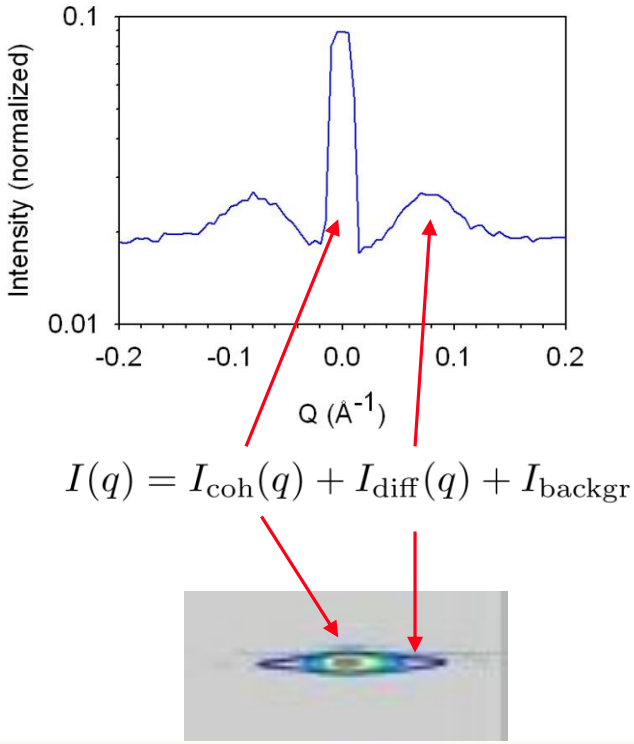

Time-resolved diffuse x-ray scattering

- Length-scale increases with substrate temperature at fixed dwell time
- Length scale increases with dwell time at fixed substrate temperature
- Need to understand the formation of a single layer

Diffuse scattering after a single laser shot

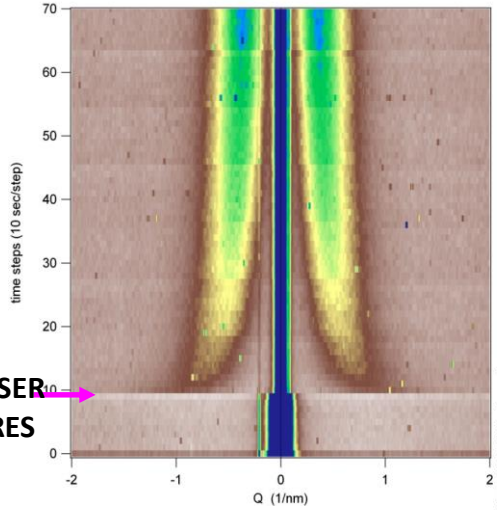

$$l(t) \propto t^n$$

n = coarsening exponent

$n = \frac{1}{3}$ diffusion-limited kinetics

$n = \frac{1}{2}$ attachment-limited kinetics

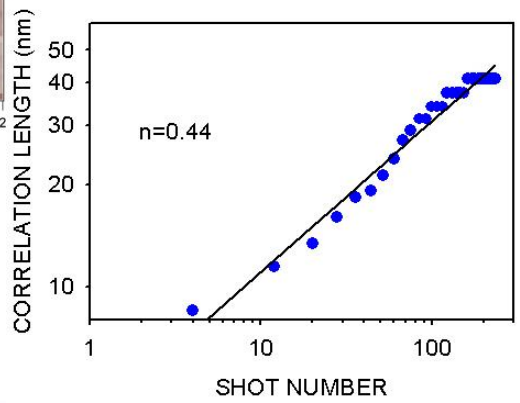

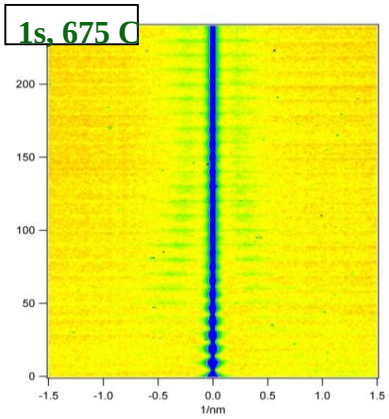

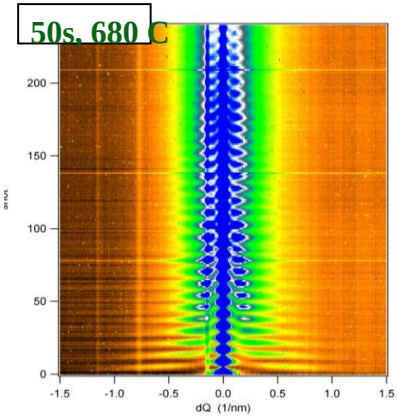

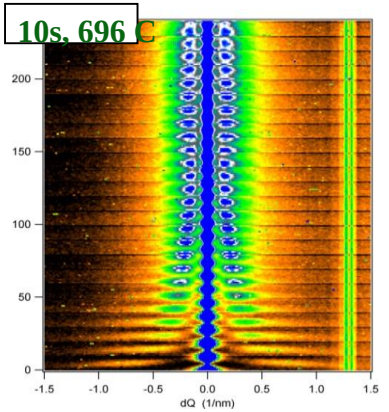

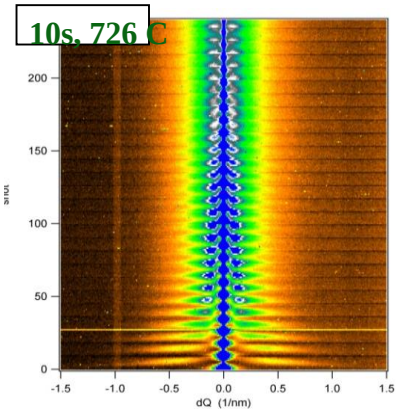

Real space imaging

- Length-scale increases with substrate temperature at fixed dwell time
- Length scale increases with dwell time at fixed substrate temperature

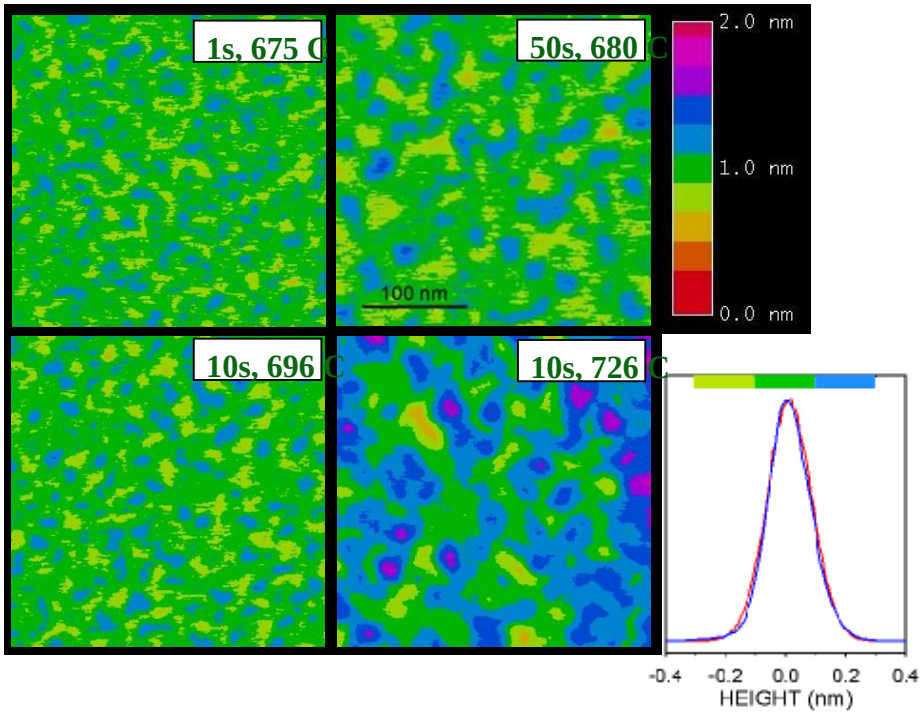

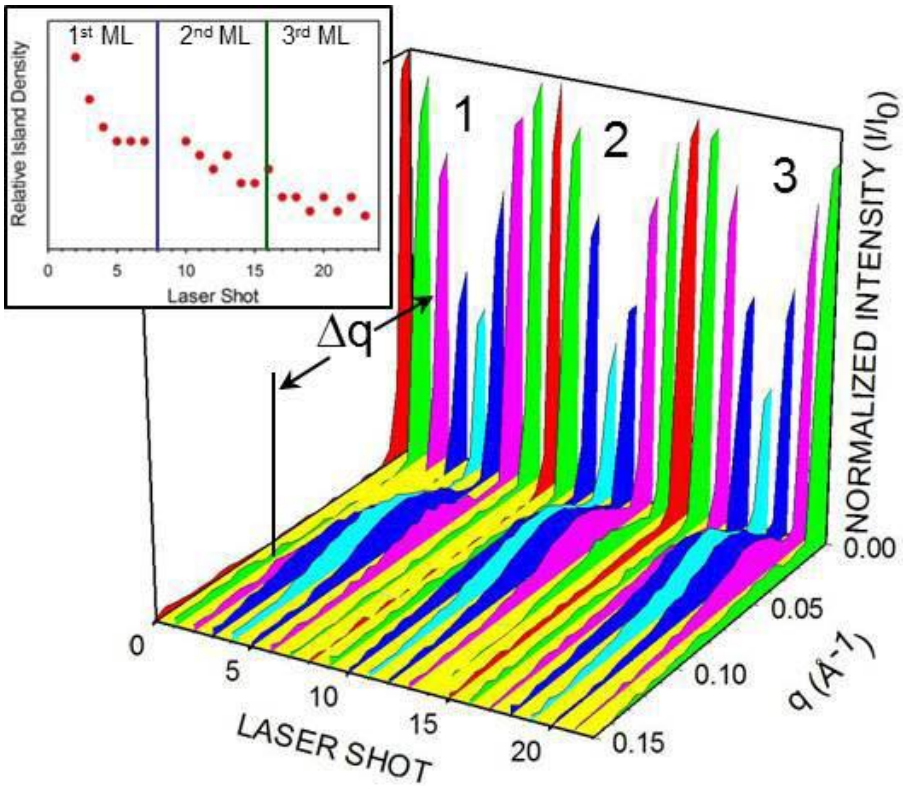

What have we learned about PLD growth?

- Pulsed Growth permits separation of thermal & non-thermal effects
- In PLD, most of the material crystallizes in first few μs
- The thermal annealing affects less than 5 - 20% of the material deposited
- Stable 2-Layer growth established for SrTiO3
- The transverse length scale depends upon Temperature and the dwell time between laser shots.
- Traditional models miss most of the physics.

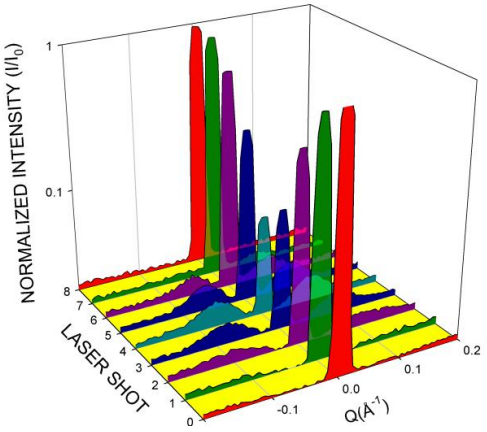

Tischler, et.al. *Phys Rev Lett* **96** (22) 226104 (2006)

X-ray Reflection Interface Microscopy (XRIM)

- Rather than measure the CTR intensity, imaging the scattered beam gives rise to interface microscopy
- Strong contrast (~100%), but weak reflected beam intensity ($R < 10^{-5}$)
- Sub-nm vertical sensitivity, but modest lateral resolution (~50-100 nm)
- Analogous to dark field imaging

Phase contrast mechanism:

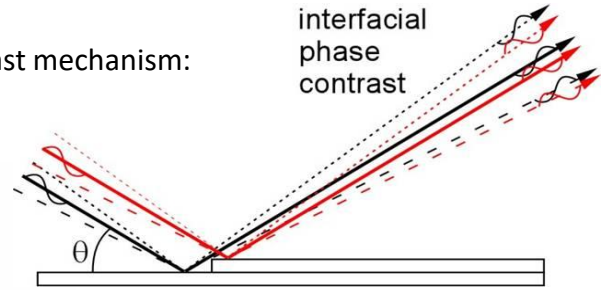

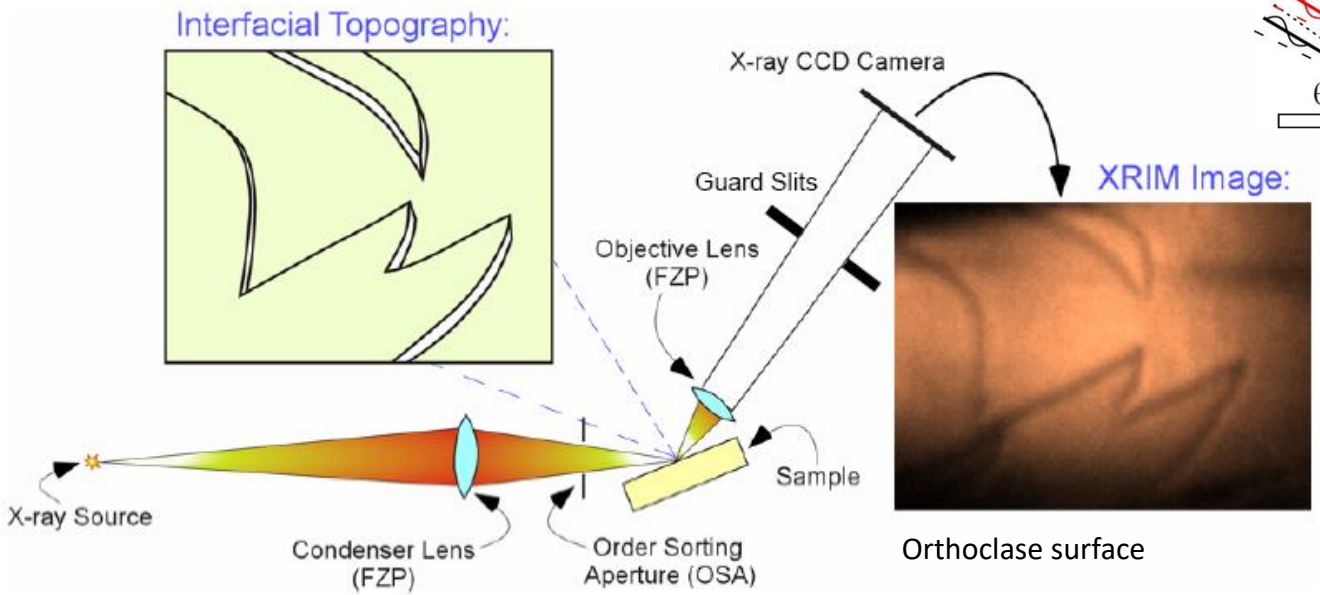

Orthoclase surface

Intensity contrast at defects:

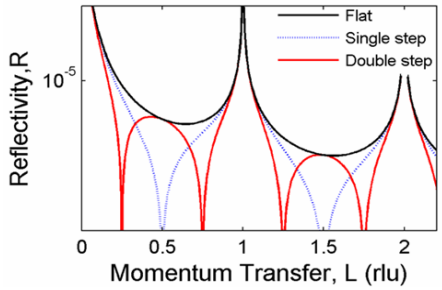

Fenter et al., *Nature Physics* 2(10) 700-704 (2006)

XRIM dissolution of calcite surface

- Mineral dissolution under constant irradiation. Scale bar is 3 µm and time stamp is the experimental time

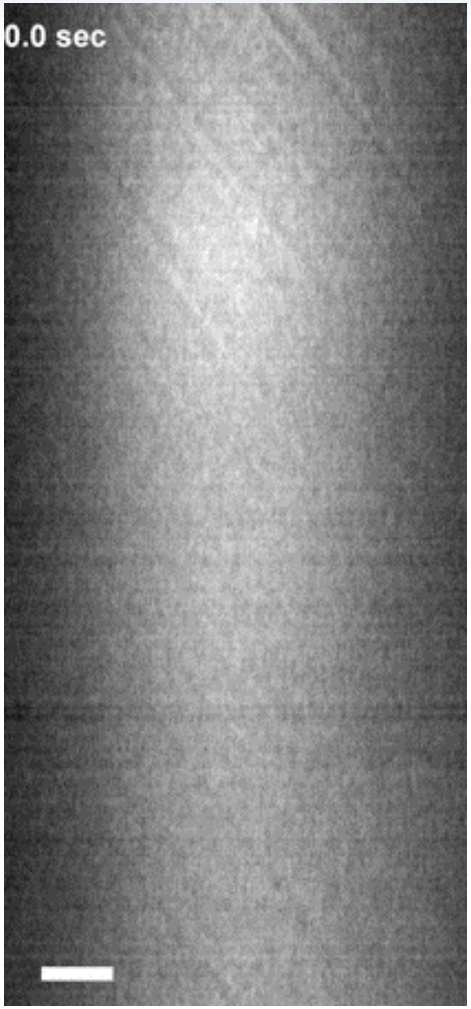

X-ray–driven reaction front dynamics at calcite-water interfaces. Nouamane Laanait, Erika B. R. Callagon, Zhan Zhang, Neil C. Sturchio, Sang Soo Lee, Paul Fenter. *Science* 18 Sep 2015: Vol. 349, Issue 6254, pp. 1330-1334

XRIM from buried interfaces

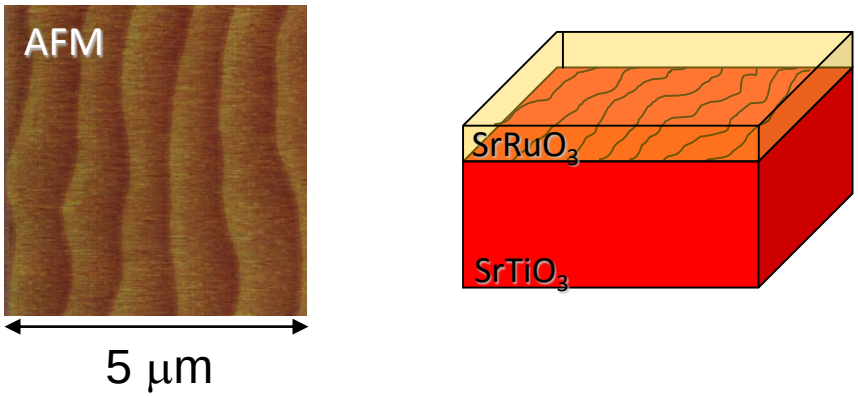

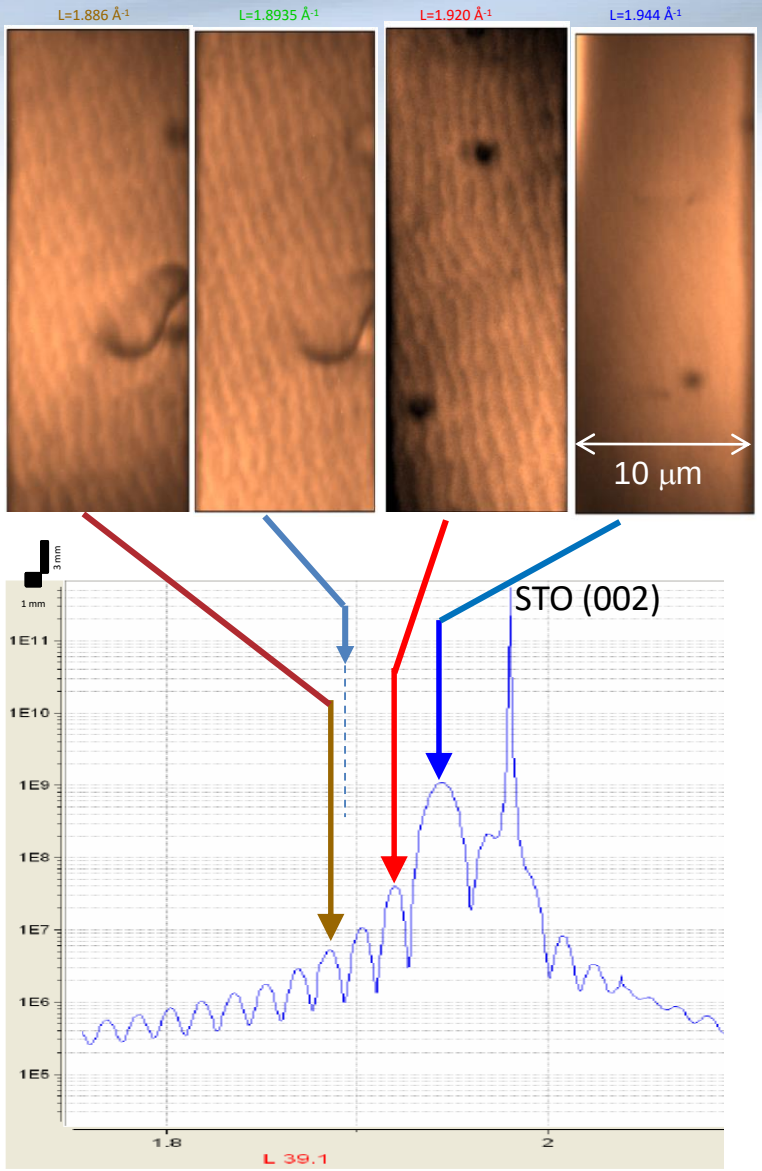

- In a thin-film, thickness fringes carry information concerning the details of the top and bottom surface (interface)
- XRIM can be applied to spatially resolve features from thin-film surface and interface structures.

Zhang, Zschack, Fenter. Nuclear Instruments and Methods in Physics Research A 649 (2011) 188–190

XRIM images of an interface between $SrRuO_3$ and $SrTiO_3$

XRIM in Thin-Films: $EuTiO_3/SrTiO_3$

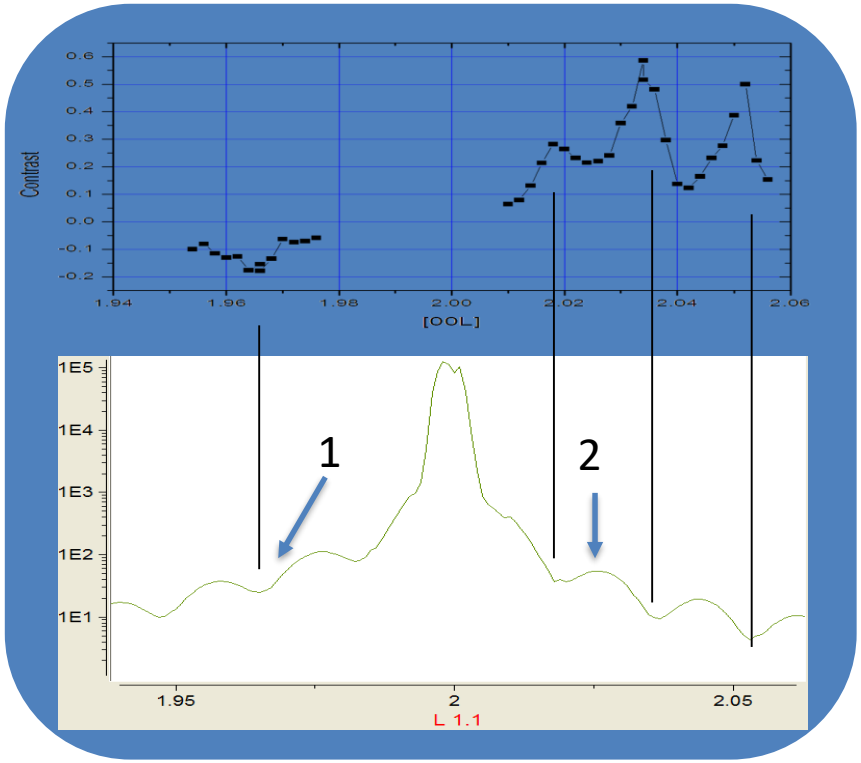

- Contrast observed in these films: phase separation or inhomogeneous strain

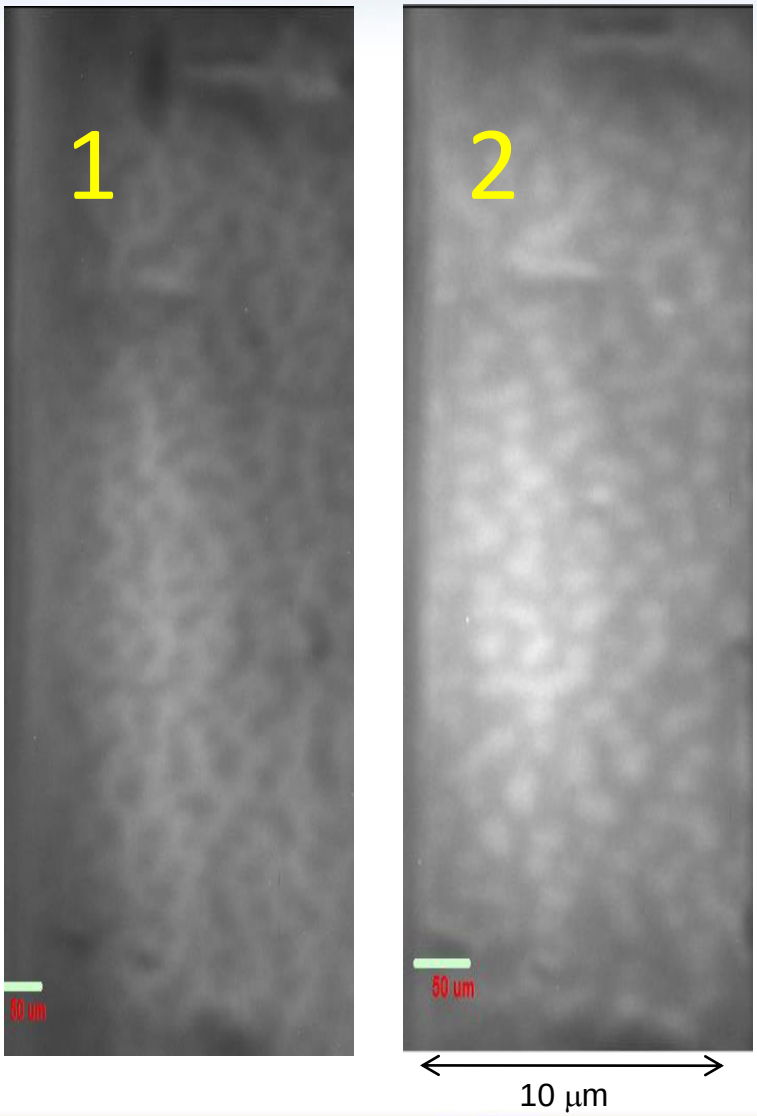

What have we learned from XRIM?

- XRIM holds great promise for in-situ real-time visualization (real-space) during materials growth and during chemical processes
- Sub-nanometer sensitivity to interface structures (normal) and 50 nm lateral spatial resolution expected.
- Value in combining both scattering (reciprocal space) with imaging (real space)

Coherent diffraction imaging of surface structures

-robust phasing transforms scattering data to microscopic images

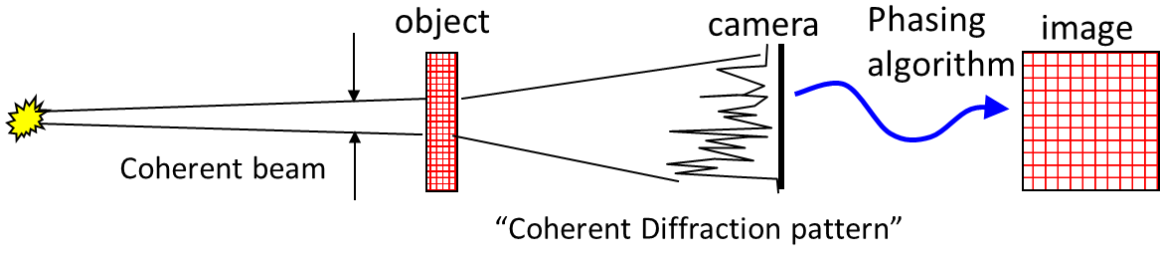

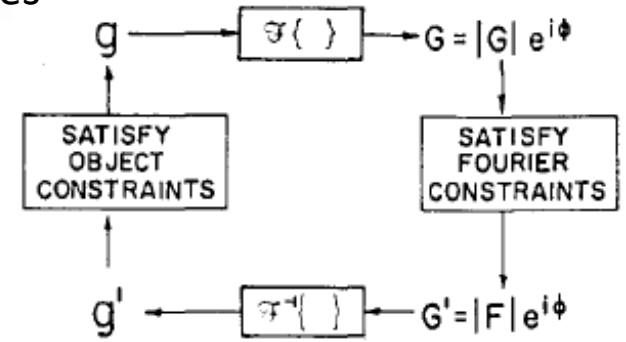

Fienup, Opt. Lett. 3, 27 (1978)

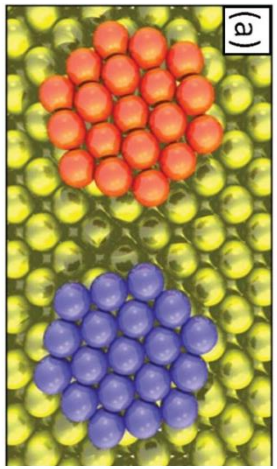

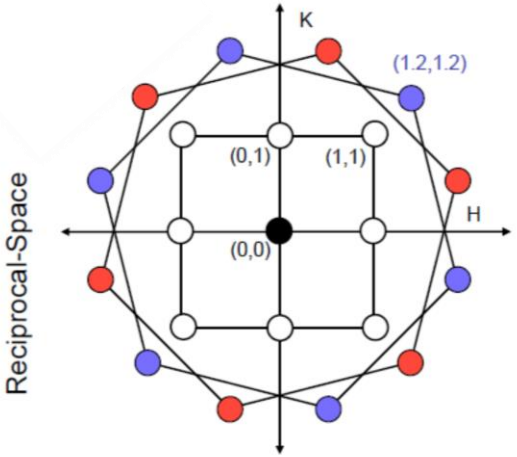

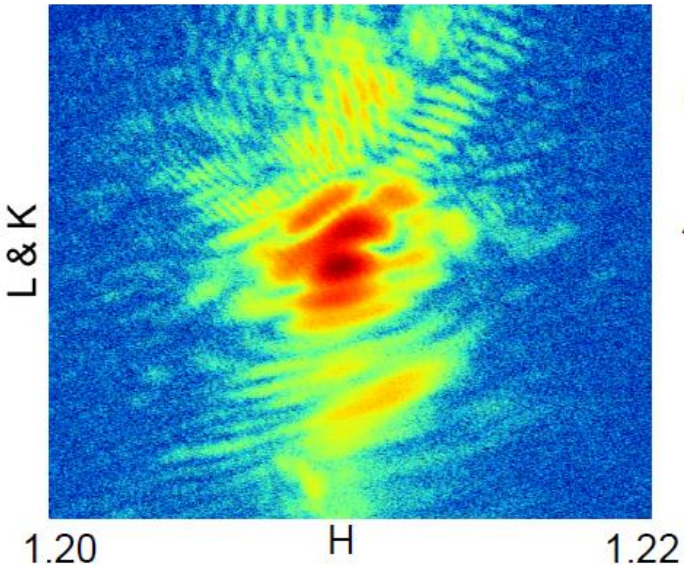

Au(001) Hexagonal reconstruction peak:
Pierce et al., unpublished results (2008)

Coherent diffraction imaging of steps on Pt (111)

- Ptychography demonstrated to image step features on Pt (111) surface using coherent diffraction imaging at the anti-Bragg specular CTR

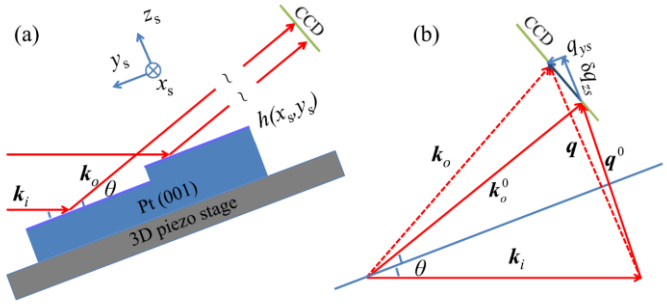

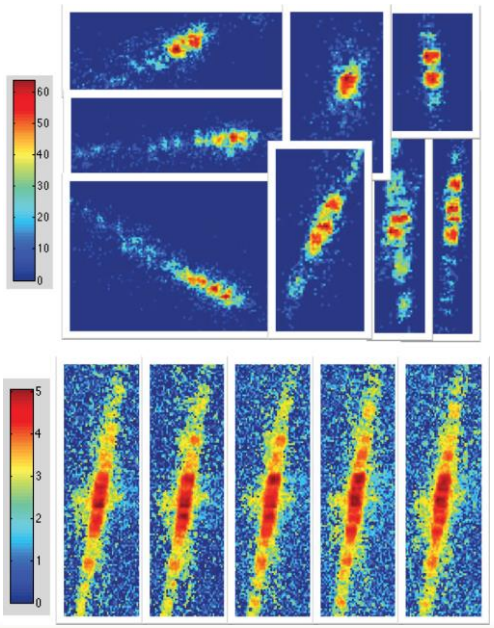

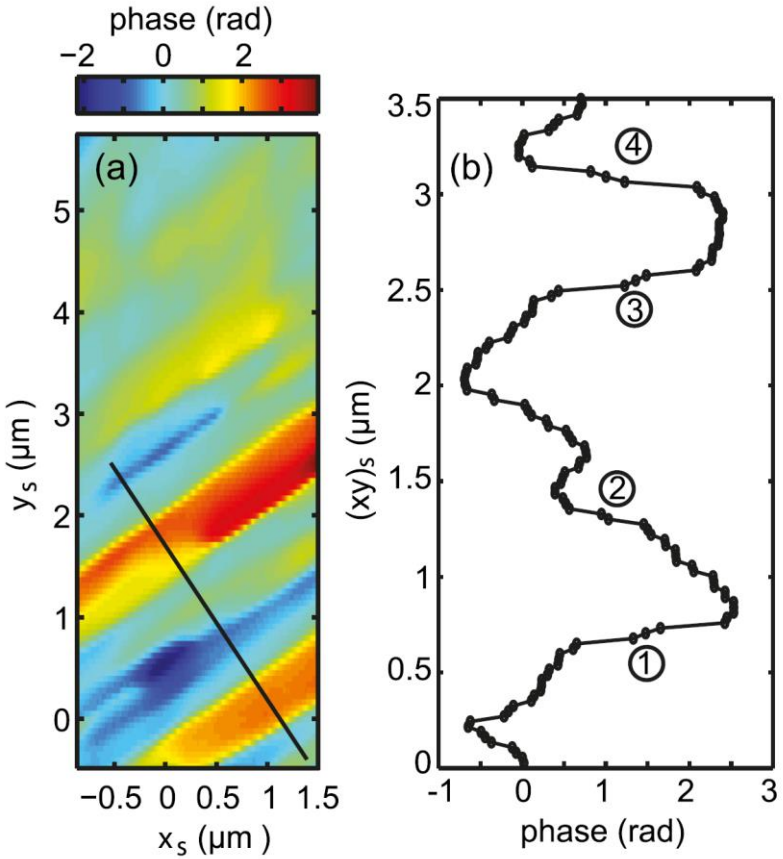

Zhu et al. Appl. Phys. Lett. 106, 101604 (2015)

Surface dynamics studied with XPCS - Au (001)

- Photon Correlation Spectroscopy exploits x-ray coherence to provide insight into surface dynamics

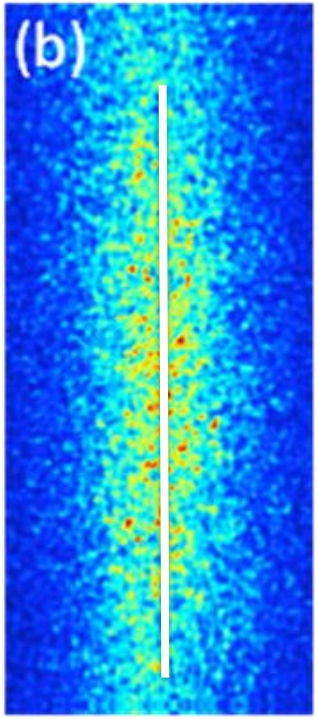

Au (001) CTR
(Anti-Bragg)

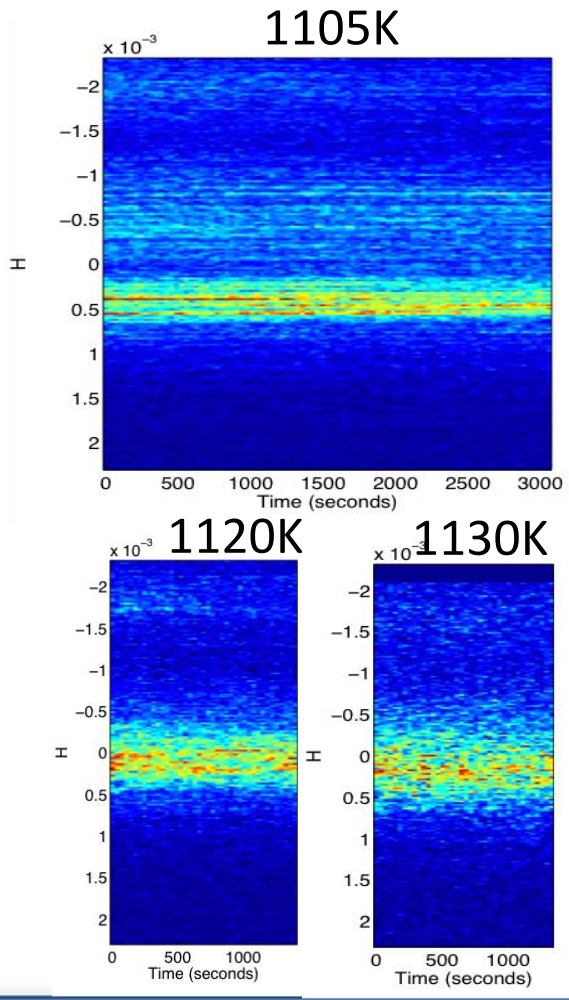

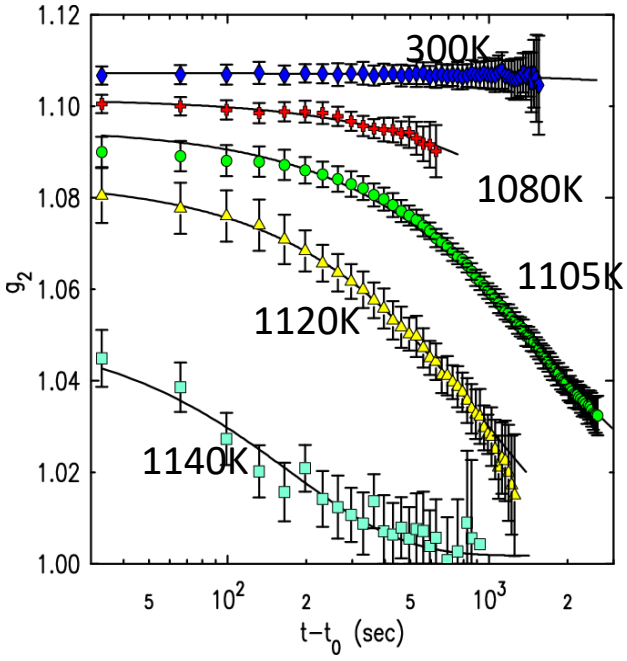

Pierce, et al., PRL 103, 165501 (2009)

Persistent oscillations of x-ray speckles: Pt (001) step flow

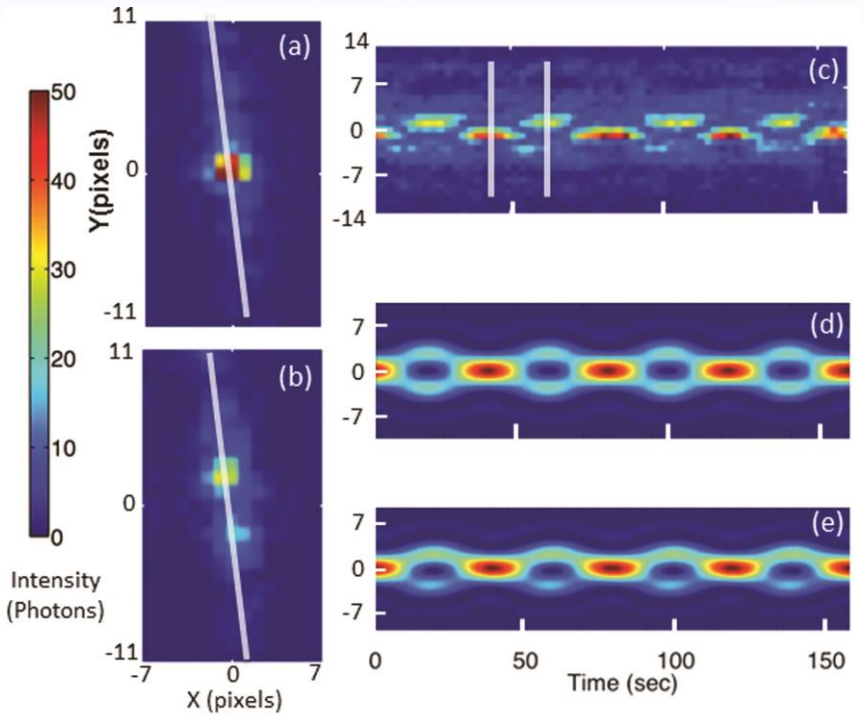

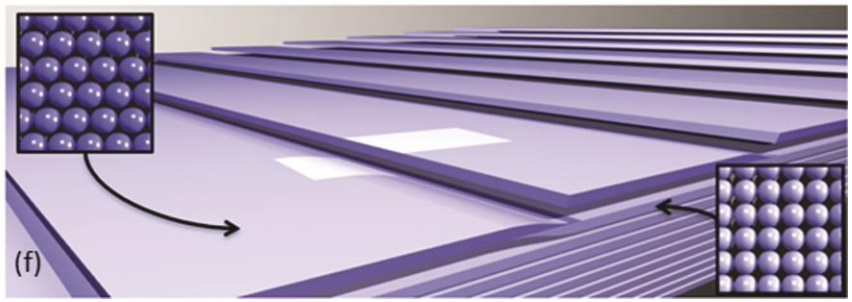

- In reflection XPCS, the exponentially decaying or under-damping autocorrelations of speckle patterns represent the time evolution of the surface reconfiguration.
- Autocorrelations from the Pt (001) surface, however, can show persistent oscillations lasting many tens of cycles without explicit heterodyning.
- Calculated intensity vs. time for the single step model (e) with the reconstructed terraces matches the observed behavior.

M. S. Pierce, D. C. Hennessy, K. C. Chang, V. Komanicky, J. Strzalka, A. Sandy, A. Barbour, and H. You. *Appl. Phys. Lett*. **99**, 121910 (2011)

Instrumentation

- Integrated diffraction – UHV growth chambers
  - Including RHEED, AUGER, LEED, XPS, sputtering, elipsometry, etc…
- Liquid spectrometers
- Small Be dome environment
- Flow cells

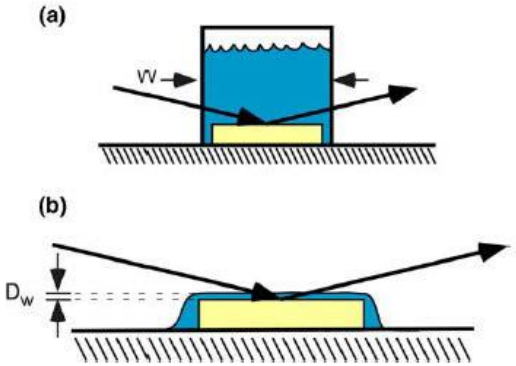

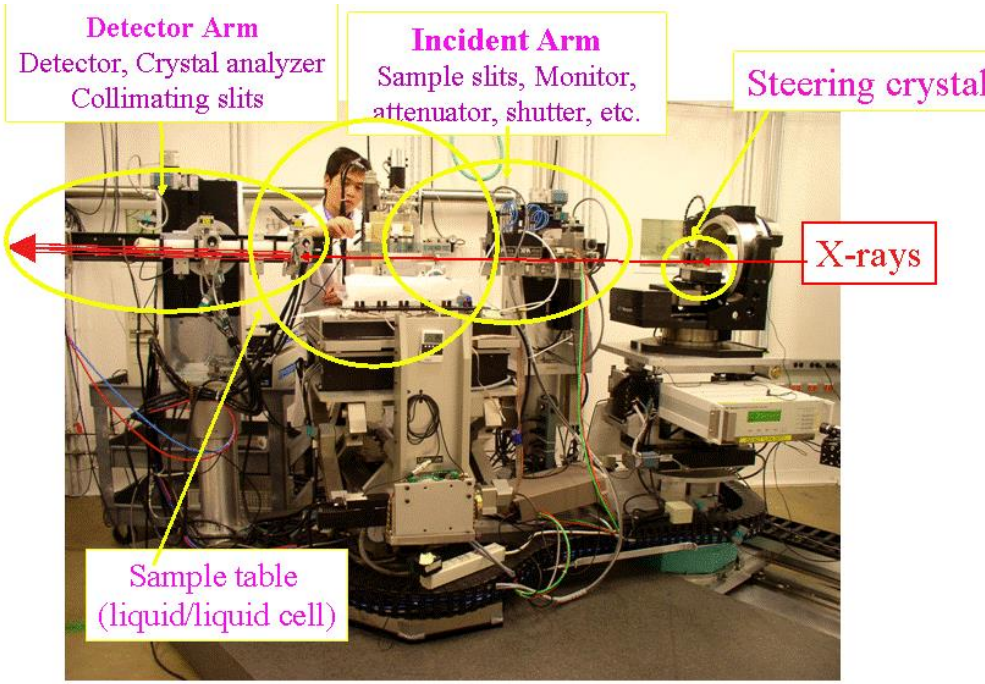

Liquid surface spectrometer

Interface Science facilities at the APS

13-ID surface scattering

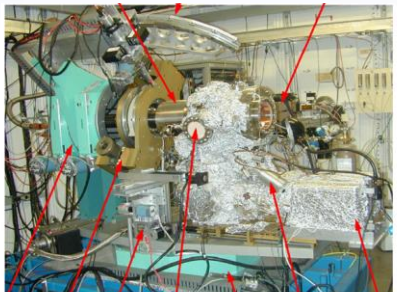

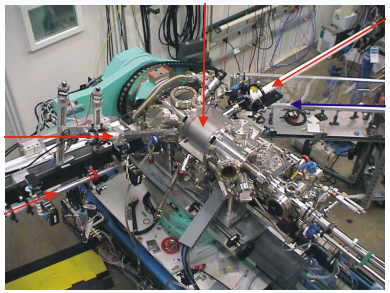

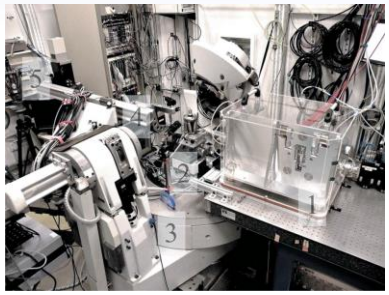

33-ID surface scattering , MBE, PLD, XRIM

MBE-2

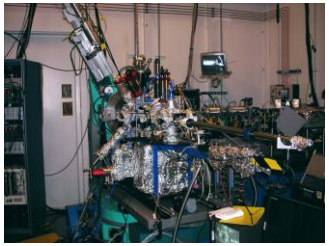

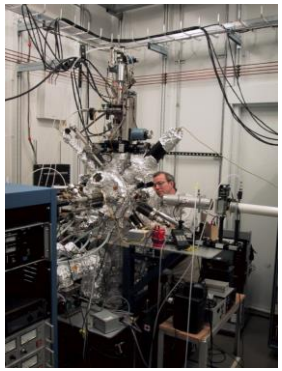

MBE-1

20-ID surface spectroscopy & diffraction

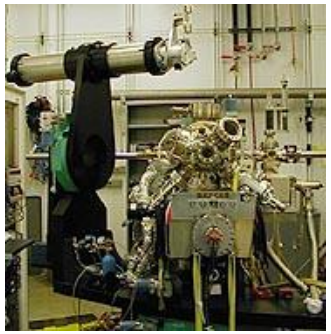

5 ID-C surface science chamber

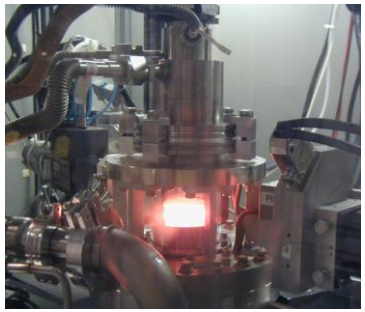

12-ID surface scattering & MOCVD

Most major Light Source facilities host interface science

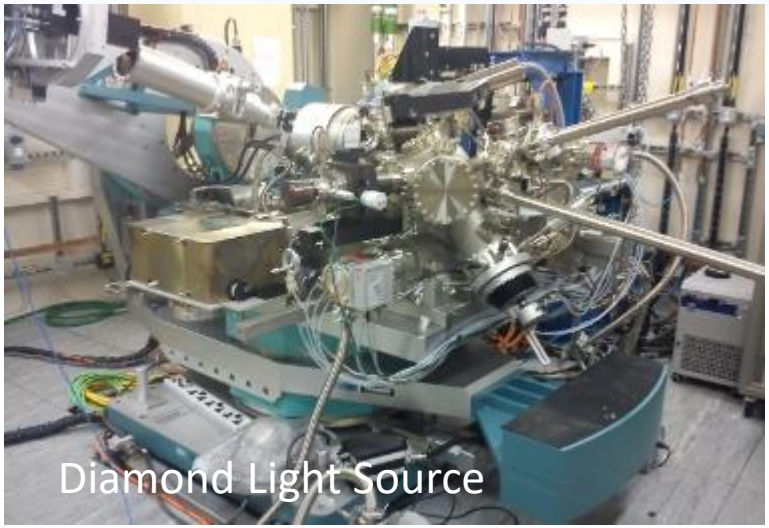

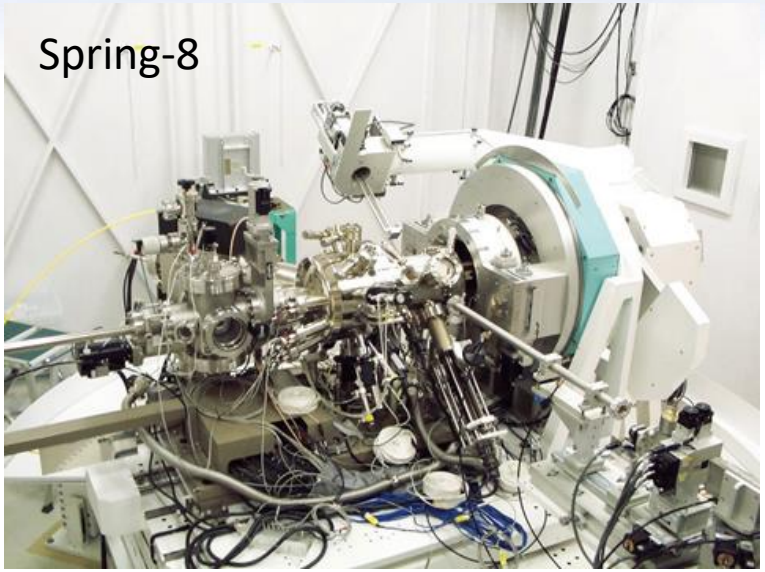

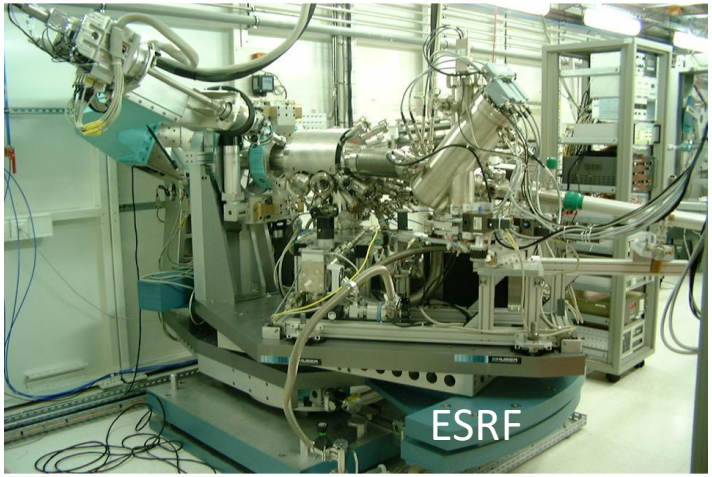

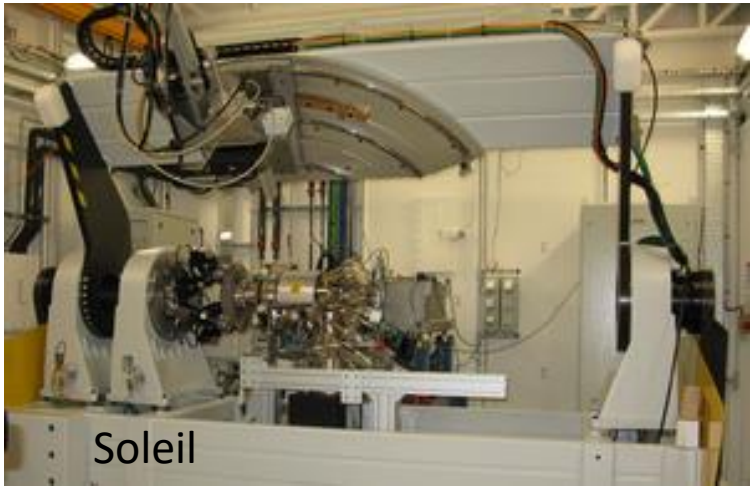

Small chamber approach (SLS & ESRF & APS)

- Ambient Chamber
- UHV baby Chamber
- Cryochamber
- High temperature system

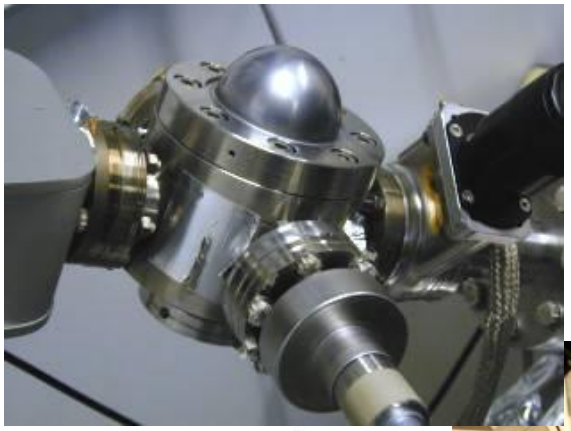

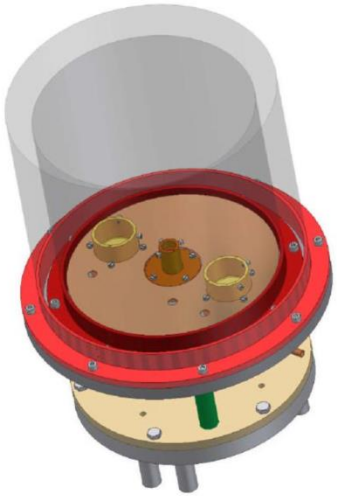

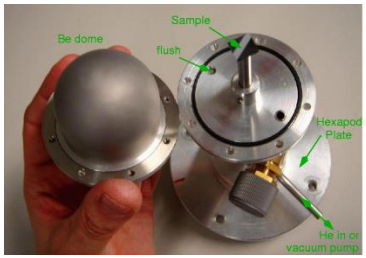

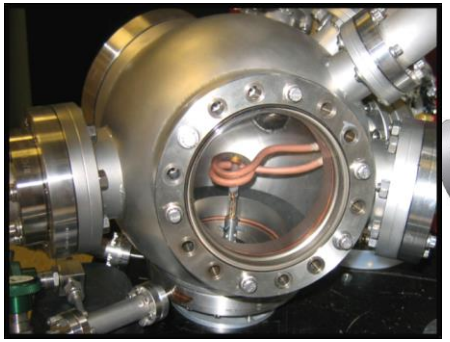

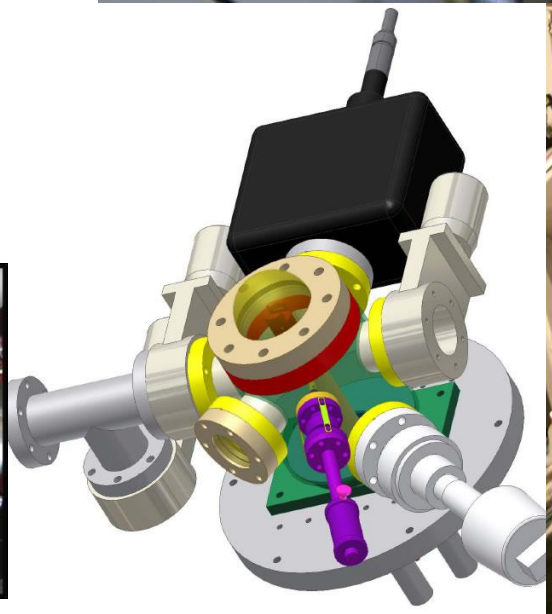

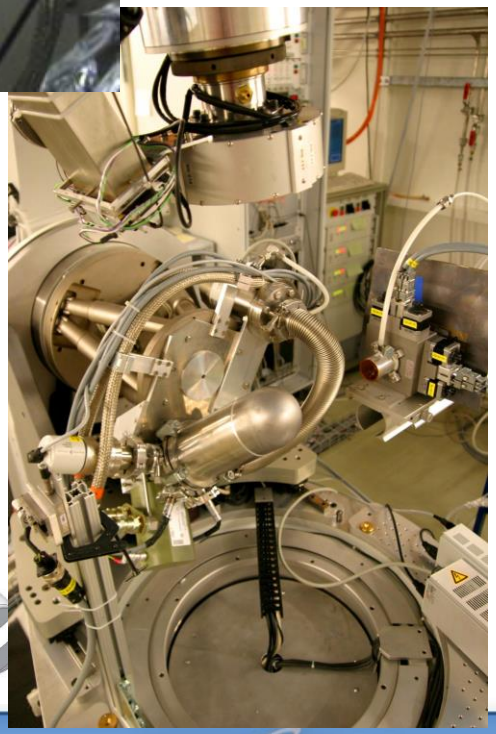

General diffractometers with sample environments

- Standardized interfaces interchangeable amongst diffractometers
- Environments include UHV, high-temperature, cryogenic, liquid flow-cells
- Enhanced general diffraction capabilities

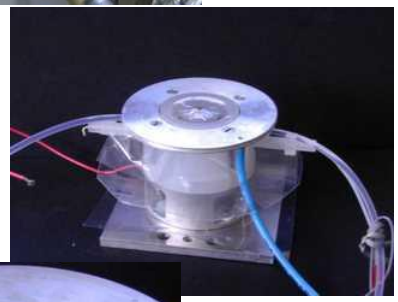

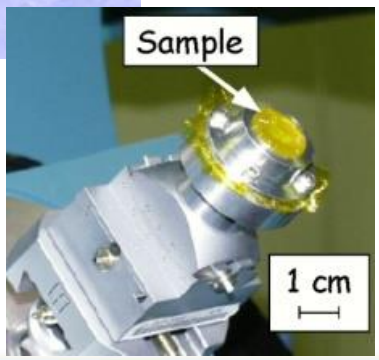

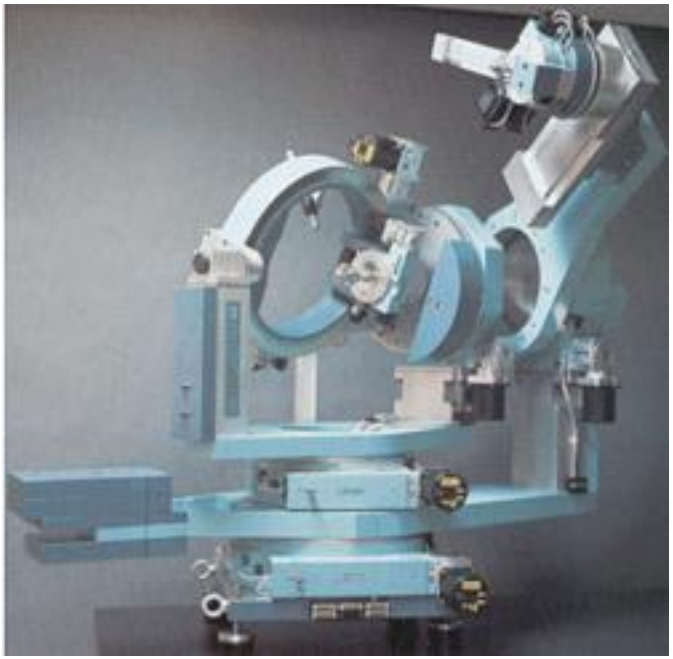

Sample environments to support interface science

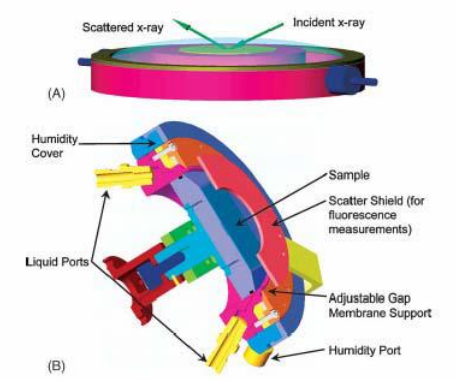

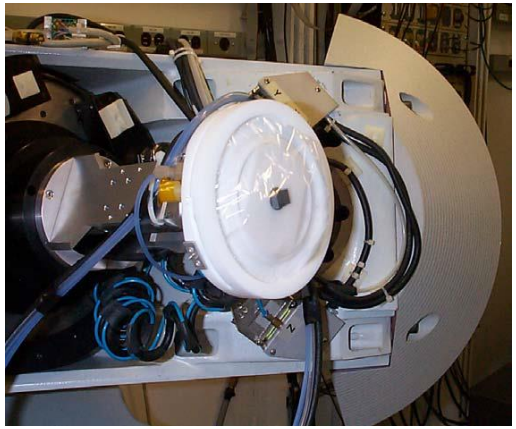

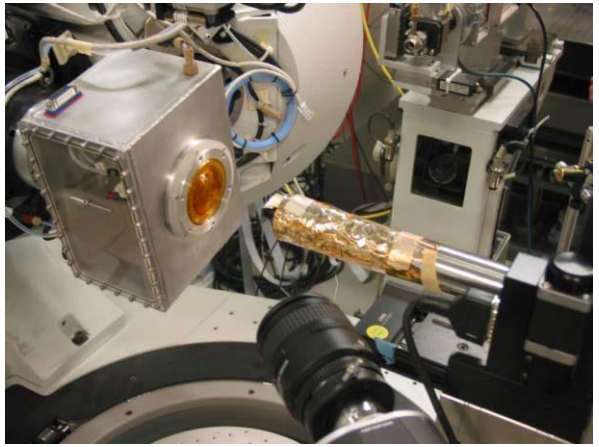

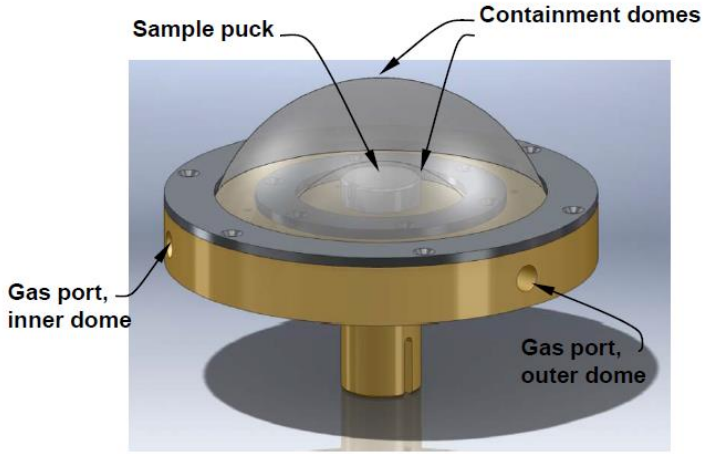

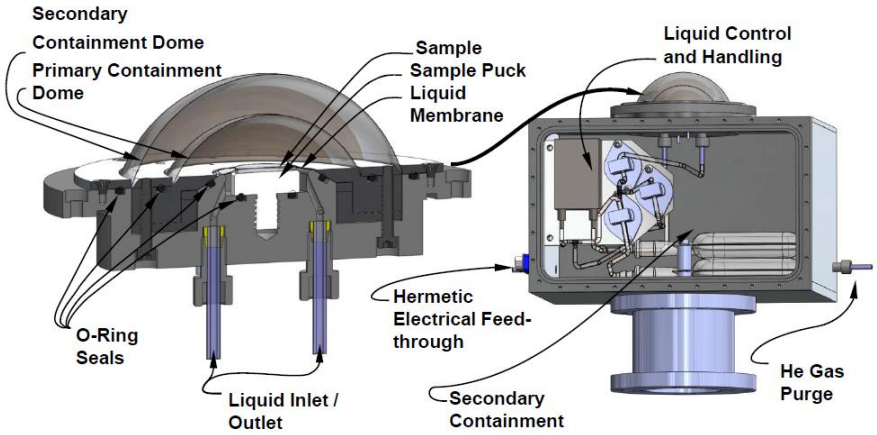

Schmidt, Eng, Stubbs, Fenter, and Soderholm (2011) Rev. Sci. Inst. 82:075105

Summary

- The origin of the Crystal Truncation Rod is the sharp termination of a lattice
- Crystal Truncation Rod scattering provides excellent sensitivity to surfaces and interfaces
- Widely diverse scientific communities exploit CTR techniques (materials synthesis, geosciences, catalysis, high-strength materials, electrochemistry)
- Learned how CTR scattering can be used to locate adsorbed species
- Demonstrated how time resolved CTR scattering can be used to study materials growth
- The CTR provides x-ray contrast that is sensitive to surface/interfaces and this scattering can be imaged with XRIM
- Many advanced techniques applied to bulk materials can be applied to interfaces through exploitation of the CTR (XPCS, CDI, diffuse scattering)